Apical actin filament turnover mediated by cyclase-associated protein is required for organization of non-centrosomal microtubules in epithelium

Running title: Dense Apical Actin excludes Microtubules

Arathi Preeth Babu[1,2], Sachin Muralidharan[1], Konstantin Kogan[1], Tommi Kotila[1], Ville Hietakangas[1,2], Jaakko Mattila[2], Minna Poukkula[1,2]*

Affiliations

1 Institute of Biotechnology, University of Helsinki, Helsinki 00790, Finland.

2 Faculty of Biological and Environmental Sciences, University of Helsinki, Helsinki 00790, Finland.

* Corresponding author: minna.poukkula@helsinki.fi

Keywords:

Epithelial cells, cytoskeleton, actin, microtubules, actin turnover, *Drosophila*

ABSTRACT

Epithelial cells rely on the precise coordination of actin and microtubule cytoskeletons to maintain their polarized structure and function. Within polarized epithelial cells, microtubules form longitudinal non-centrosomal arrays essential for organelle positioning and facilitate directional cargo trafficking whereas the apical actin cytoskeleton supports cell shape and tissue architecture. This study investigates the interplay between disrupted apical actin dynamics and microtubule organization *in vivo* within *Drosophila* epithelial tissue. Loss of actin turnover promoting Cyclase-Associated Protein (CAP) results in the excessive accumulation of stable actin structures at the apical cortex. We show that accumulated apical actin sterically excludes microtubules and membrane-bound vesicles. Consequently, non-centrosomal microtubule-dependent processes are impaired, leading to nuclear mispositioning, disrupted apical cargo transport, and defective microvilli formation in CAP mutant cells. Our findings highlight that dense apical actin, due to impaired actin turnover catalyzed by CAP, disrupts the apical organization of non-centrosomal microtubules. This suggests that spatially regulated actin filament turnover is important for microtubule organization and sustaining the polarized functions of epithelial tissues.

INTRODUCTION

Epithelia are sheets of polarized cells that line tissues and serve as protective barriers against the external environment. These cells exhibit distinct apical and basal surfaces, which enables key epithelial functions such as barrier function, absorption, secretion, and transport (Buckley & St Johnston, 2022). The establishment and maintenance of epithelial cell structure and function depend on the coordinated organization of the actin and microtubule cytoskeletons (Raman et al., 2018). Although, the roles of microtubules in supporting the polarized functions of differentiated epithelial cells are well established (Meiring et al., 2020), the interplay between the actin and microtubules in epithelial cells has been mostly studied in the context of epithelial morphogenesis (Röper, 2020).

The dense apical actin cytoskeletal network is essential for maintaining epithelial cell shape, tissue architecture, and mechanical integrity (Pelaseyed & Bretscher, 2018). The apical, and junctional actomyosin networks, comprising of contractile actin filaments and myosin-2, are key forces driving epithelial morphogenesis (Martin et al., 2009; Roh-Johnson et al., 2012). Additionally, apical actin also supports vesicle trafficking, junctional organization, and cell–cell adhesion. Many epithelial cells feature actin-rich apical structures such as microvilli or stereocilia, that are crucial for tissue functions like nutrient absorption and sensory perception (Sauvanet et al., 2015; Sharkova et al., 2023). The biogenesis of apical microvilli relies on the intracellular apical transport and delivery of membrane vesicles and cargos such as microvilli-specific cadherin PCDH15 / *Drosophila* Cad99C along non-centrosomal microtubules and apical actin network. Defects in this process disrupt microvillar formation (D'Alterio et al., 2005; Khanal et al., 2016; Knowles et al., 2014).

In most epithelia, microtubules are organized into non-centrosomal arrays with their minus-ends anchored at the apical cortex and plus-ends extending toward the basal side (Bartolini & Gundersen, 2006; Meads & Schroer, 1995; Mogensen & Tucker, 1987; Perrin & Matic Vignjevic, 2023; Toya & Takeichi, 2016). This polarized arrangement supports directional trafficking by dynein and kinesin motor proteins, enabling the targeted delivery of vesicles and organelles to apical and basolateral membrane domains, respectively (Kreitzer & Myat, 2018; Reck-Peterson et al., 2018). During epithelial morphogenesis longitudinal microtubule arrays are coordinated with actomyosin contractility (Booth et al., 2014a; Ko et al., 2019a; J.-Y. Lee & Harland, 2007; Singh et al., 2018, 2024; Zhou et al., 2010) The establishment of the non-centrosomal microtubule arrays depends on the apical anchoring of microtubule minus-ends, a process that requires coordinated action of the microtubule-associated proteins CAMSAP3/ *Drosophila* Patronin, and ACF7/MACF1/ *Drosophila* spectraplakin Shot, as well as the apical spectrin cytoskeleton (Khanal et al., 2016; Muroyama et al., 2018; Nashchekin et al., 2016; Ning et al., 2016; Noordstra et al., 2016; Toya et al., 2016). CAMSAP3/Patronin binds, stabilizes, and anchors the minus ends of microtubules at the apical cortex (Goodwin & Vale, 2010; Toya et al., 2016). Shot (ACF7/MACF1) crosslinks microtubules to the actin cytoskeleton, aiding in the

assembly and maintenance of non-centrosomal microtubule arrays (Applewhite et al., 2010; S. Lee & Kolodziej, 2002).

It has become increasingly clear that actin and microtubule cytoskeletons interact and are coordinated (Pimm & Henty-Ridilla, 2021). Studies conducted *in vitro* and in cultured cells have revealed that actin structures actively modulate microtubule dynamics and organization over time and space. In particular, the organization and density of filamentous actin not only supports cellular architecture but also has direct consequences for microtubule dynamics and organization, for instance at the leading edge of migrating cells and regulating centrosomal microtubule nucleation during mitosis (Ballestrem et al., 2000; Colin et al., 2018; Farina et al., 2019; Gélin et al., 2023; Gupton et al., 2002; Gupton & Waterman-Storer, 2006; Inoue et al., 2019; Waterman-Storer & Salmon, 1997). This cytoskeletal interplay is especially important for the regulation of cell shape and polarity in migrating cells, and during epithelial morphogenesis (Ko et al., 2019b; Priya, 2022; Ricolo & Araújo, 2020), as well as neuronal and epithelial cells (Dogterom & Koenderink, 2019). However, how regulation of actin dynamics affects structural organization of actin and actin-microtubule coordination, needs to be explored especially in the context of epithelial cell functions *in vivo*.

In this study, we utilize the *Drosophila* follicular epithelium as a model system to investigate the critical role of actin dynamics in the organization and function of non-centrosomal microtubules. Our study demonstrates that actin disassembly protein, Cyclase associated protein-mediated apical actin turnover is required for correct organization of non-centrosomal microtubule arrays in the *Drosophila* follicular epithelium. We show that actin accumulation in CAP deficient cells leads to steric exclusion of non-centrosomal microtubule arrays apically, causing mispositioning of cell nuclei and impairment of apical cargo trafficking crucial for microvilli biogenesis. Together, these findings highlight the importance of actin dynamics for establishment and maintenance of non-centrosomal microtubules and supporting polarized function and structure of epithelial cells.

RESULTS

Apical and basal actin filaments are under high turnover in follicular epithelium

To investigate the role of actin dynamics in epithelial cells, we treated *Drosophila* egg chambers (Figure 1 A) with 20 µM Latrunculin A (Lat A). Lat A sequesters actin monomers thus inhibit their polymerization to filamentous actin (Spector et al., 1983). Lat A treatment can be used to monitor the stability of already existing actin filaments. In follicular epithelial cells, Lat A treatment resulted in the disappearance of apical and basal actin, whereas cortical actin remained largely unaffected in both stage 8 and 10 egg chambers (Figure 1B). This suggests that apical and basal actin in follicle cells are under rapid turnover. To investigate the role of apical actin turnover in epithelial

cells, we focused on Cyclase-associated protein (CAP aka *Drosophila* Capt), a regulator of actin dynamics. CAP is a well-known actin-binding protein, which promotes rapid actin turnover via its multiple biochemical functions: depolymerization of cofilin-decorated actin filaments, followed by cofilin release and the subsequent recharging of “old” actin monomers by exchanging bound nucleotides from ADP to ATP (Kotila et al., 2018; Lappalainen et al., 2022; Ono, 2013). Notably, loss of CAP leads to an excessive accumulation of filamentous actin specifically at the apical side (Baum & Perrimon, 2001) of *Drosophila* follicular epithelial cells (Figure 1 C; Supl. Figure 1 A). Moreover, Latrunculin A treatment revealed that the accumulated dense actin of CAP mutant cells was very stable as it persisted even after prolonged (2 h) Latrunculin A treatment (Figure 1 D & E).

Despite highly localized accumulated actin, CAP protein itself displayed mostly diffuse cytoplasmic localization (Supl. Figure 1 A). In other systems (Bertling et al., 2004; Ono, 2013), CAP targets specifically those actin filament populations that are under rapid turnover. We investigated if specific actin filament configurations would be enriched in CAP mutant cells. Indeed, accumulated apical actin in CAP mutant cells displayed increased levels of proteins promoting rapid actin filament disassembly, such as Aip1 and Twinfilin (Supl. Figure 1 B, D), suggesting compensatory mechanisms for managing excess of filamentous actin. While the actin filament elongator Ena was enriched in these actin structures (Supl. Figure 1 E; Baum & Perrimon, 2001), profilin, which supplies monomeric actin for elongation, was expressed at higher levels but was not localized at the site of actin accumulation (Supl. Figure 1 C). This indicates that an excess of actin filament assembly is unlikely to occur at the apical side of CAP mutant cells. Additionally, α-actinin and tropomyosin were enriched at the site of actin accumulation (Supl. Figure 1 F-G), whereas active non-muscle myosin II was either partially or completely excluded from apical actin networks in a stage-dependent manner, suggesting that the accumulated actin is unlikely to form contractile actomyosin filaments (Supl. Figure 1 H, H’). In conclusion, the dense and stabilized actin in CAP mutant cells is composed of a complex mixture of filamentous actin and various actin-binding proteins but appears to lack components providing contractile properties.

Nucleotide exchange activity of CAP is required for maintaining proper apical actin dynamics

CAP is a multidomain protein, with each domain exhibiting distinct biochemical activities that contribute to actin turnover (Figure 2 A). The N-terminal Helical Folded Domain (HDF) enhances depolymerization of cofilin-decorated actin filaments by dissociating cofilin-actin monomers (Bertling et al., 2004; Chaudhry et al., 2013; Jansen et al., 2014; Kotila et al., 2019; Quintero-Monzon et al., 2009; Shekhar et al., 2019). The Polyproline (PP) domain binds profilin (Bertling et al., 2007). The Wiskott-Aldrich Syndrome Protein Homology 2 (WH2) domain interacts with both ADP-actin and ATP-actin monomers (Bertling et al., 2007; Freeman et al., 1995; Lila & Drubin,

164 1997; Mattila et al., 2004). The CARP domain binds ADP-actin monomers and
165 facilitates nucleotide exchange from ADP to ATP, thereby recharging actin monomers
166 for polymerization (Bertling et al., 2004; Kotila et al., 2018; Moriyama & Yahara, 2002).

167 The existing biochemical, structural, and cell biological studies have contributed to a
168 comprehensive understanding of how CAP's biochemical activities are orchestrated to
169 promote actin turnover. Therefore, to understand how CAP mediates apical actin
170 turnover *in vivo*, we generated mutant constructs targeting critical amino acids in the
171 HFD, PP, WH2, and CARP domains (Figure 2 A, Table 1) and tested the ability of these
172 constructs to rescue the CAP mutant phenotype. Our results show that CAP constructs
173 with mutations in HFD, PP, and WH2 domains rescued the actin accumulation
174 phenotype in stages 8-10 of oogenesis (Supl Figure 2 B-E). However, the CARP
175 domain mutant did not rescue actin accumulation in the CAP mutant cells even in
176 stages 9-10 (Figure 2 B-D). This result shows that the nucleotide exchange activity of
177 CAP is most critical for efficient apical actin turnover. Our observation is consistent
178 with the fact that nucleotide exchange is the most conserved function of CAP across
179 eukaryotes (Ono, 2013) and its loss leads to significant actin accumulation in yeast
180 (Kotila et al., 2018). Another established nucleotide exchange factor for actin is profilin,
181 and in budding yeast the loss of CAP can be rescued by over-expression of profilin
182 (Vojtek et al., 1991). However, in CAP mutant follicle cells over-expression of profilin
183 did not rescue apical actin accumulation (Figure 2 E). The failure of profilin
184 overexpression to rescue the CAP mutant phenotype suggests that merely increasing
185 nucleotide exchange is not sufficient to restore proper actin dynamics in these cells,
186 indicating a more complex regulatory mechanism at play. Surprisingly, a rescue
187 construct with mutations in the N-terminal domain (responsible for promoting the
188 depolymerization of cofilin-decorated actin filaments) effectively rescued the CAP
189 mutant phenotype. Efficient actin depolymerization typically requires multimerization
190 mediated by the CAP N-terminus (Chaudhry et al., 2013). However, *Drosophila* CAP
191 lacks the critical N-terminal sequence for multimerization (Benlali et al., 2000), which
192 may explain this finding. In conclusion, our findings highlight the critical role of CAP's
193 nucleotide exchange activity in regulating actin dynamics particularly in the apical
194 region.

195

196 **CAP mutant cells display abnormal distribution of membrane-bound organelles**
197

198 In our experiments we used MARCM system with mCD8-GFP as a clonal marker to
199 outline the mutant cells in chimeric tissues (T. Lee & Luo, 2001). The membrane-bound
200 mCD8-GFP labels cell membranes and apical microvilli (Blanc et al., 1988; Burr et al.,
201 2014). In follicle cells, mCD8-GFP marks also the entire cytoplasm, possibly
202 highlighting the enrichment of endomembrane compartments in these cells.
203 Interestingly, in CAP mutant cells mCD8-GFP-labeled compartments were lost at the
204 regions of actin accumulation (Figure 3 A). The phenotype was rescued by
205 reintroducing wild-type CAP (Figure 3 B). This result suggests that accumulated actin
206 causes significant impairment in the normal distribution of endomembrane

207 components in CAP mutant cells. Moreover, we found that the site of actin
208 accumulation was devoid of membrane-bound organelles, indicated by the absence
209 of specific markers for the endoplasmic reticulum (ER marker calnexin Cnx99A) and
210 Golgi (trans-Golgi-localizing Golgin 84) (Figure 3 C, D). Transmission electron
211 microscopy (TEM) imaging of CAP mutant cells confirmed that the site of actin
212 accumulation lacked all membrane-bound cytoplasmic components (Figure 3 E i, ii).
213 Additionally, CAP mutant cells displayed ectopic electron-dense vesicular structures
214 both beneath and surrounding the site of actin accumulation (Figure 3 E iii, iv). Notably,
215 also Gutzeit, (1986) described appearance of electron-dense structures in follicle cells
216 upon disruption of microtubules and suggested that these vesicular structures contain
217 vitelline membrane components destined for apical secretion. Highly active apical
218 secretion by follicle cells during stages 9-10 is required for depositing extracellular
219 components and vitelline membrane proteins into the extracellular space between
220 oocyte and follicle cells. This space progressively widens to form the perivitelline
221 space, a membrane component of mature eggshell. Interestingly, the width of the
222 perivitelline space, apically to CAP mutant cells was decreased compared to the
223 neighboring cells (Figure 3 E), further providing evidence that apical secretion of
224 vitelline membrane components in CAP mutant cells was impaired. In conclusion,
225 apically accumulated dense actin in CAP mutant cells excludes endomembrane
226 cytoplasmic components and vesicles destined for apical secretion and formation of
227 perivitelline space.

228

229 **Defects in CAP-mediated apical actin turnover affect formation of apical**
230 **microvilli**

231

232 The formation of the perivitelline space begins during mid-oogenesis (stages 8–9),
233 when follicle cells develop dense apical microvilli that interdigitate with microvilli
234 projecting from the oocyte. Formation of apical microvilli has been shown to be
235 required for proper expansion of the perivitelline space (Khanal et al., 2016).
236 Therefore, we measured the length of apical microvilli and found them to be
237 significantly shorter in CAP mutant cells compared to controls or mutant cells rescued
238 with wild type CAP (Figure 4 A, B). A well-known component of follicle cell microvilli
239 and a crucial regulator of their biogenesis is protocadherin Cad99C, a *Drosophila*
240 homolog of PCDH15 (Protocadherin-15) (D'Alterio et al., 2005; Schlichting et al.,
241 2005). In wild-type cells, Cad99C was localized at the apical microvilli (Figure 4 C).
242 However, in CAP mutant cells, the localization of Cad99C at the apical surface was
243 reduced, with most of the protein retaining beneath the site of actin accumulation
244 (Figure 4 C, E-F). This result shows that the dense apical actin networks in CAP
245 mutant cells prevent trafficking of Cad99C-containing vesicles to the apical surface.
246 Cad99C is an established cargo transported by Dynein and Rab11 in follicle cells
247 (Khanal et al., 2016). Therefore, we investigated whether microtubule-based transport
248 is disrupted in CAP mutant cells. Transport of apical cargoes are mediated by the
249 microtubule minus-end-directed motor protein Dynein (Harris & Peifer, 2005; Horne-

250 Badovinac & Bilder, 2008; Reck-Peterson et al., 2018; Wilkie & Davis, 2001), which
251 carries Rab11-positive recycling endosomes toward the apical cortex, where
252 microtubule minus-ends are anchored. Rab11, a member of the RAB GTPase family,
253 is critical for polarized trafficking of various cargoes, including membrane proteins and
254 junctional components (Casanova et al., 1999; Jing & Prekeris, 2009; Roeth et al.,
255 2009). We first examined the localization of Dynein and Rab11-positive endosomes in
256 the CAP mutant follicle cells. In control cells, both Dynein and Rab11 were enriched at
257 the apical surface. However, in CAP mutant cells, Dynein and Rab11 localized beneath
258 the accumulated apical actin (Figure 4 F–H', I–K'). The localization of Rab11 beneath
259 accumulated actin suggest that trafficking of Dynein and Rab11-mediated cargoes to
260 the apical cortex is impaired by the excess apical actin in CAP mutant follicle cells. It
261 should be noted that apical trafficking of Cad99C is also mediated by Myosin V motor
262 protein along the apical actin network (Khanal et al., 2016), but our current
263 experiments do not address whether its functions are affected in CAP mutant cells.
264 Taken together, these results demonstrate that CAP-mediated apical actin turnover is
265 needed for trafficking of apical cargoes and for microvilli biogenesis.

266

267 **Excess apical actin impairs microtubule organization in epithelial cells *in vivo***

268

269 During initial characterization of CAP mutants Baum & Perrimon, 2001 did not detect
270 obvious defects in microtubules. However, experiments *in vitro* and in cultured cells
271 have revealed that organization of actin filaments can prevent or guide the growth of
272 microtubules (Colin et al., 2018; Gélin et al., 2023; Gupton & Waterman-Storer, 2006).
273 Therefore, we decided to test this possibility *in vivo* in CAP mutant epithelial cells. To
274 achieve a pronounced accumulation of apical actin, we used longer recovery time after
275 generation of mutant clones compared to that used by Baum and coworkers. We found
276 that, the apical region of CAP mutant cells, characterized by accumulated actin,
277 exhibited decreased levels of stable acetylated microtubules (Figure 5 A-B', Supl
278 Figure 3A, A') as well as α- and β-tubulin (Figure 5 C, D), indicating that microtubules
279 were excluded from the region of actin accumulation. We also analyzed microtubule
280 organization in stretch cells which are specialized flattened follicle cells. The flat
281 morphology of stretch cells enables visualization of the cytoskeleton within the whole
282 cell. In CAP mutant stretch cells, actin accumulation was predominant in one
283 cytoplasmic region, which the stable acetylated microtubules were not able to
284 penetrate (Supl Figure 3 B). Together, these findings reveal that dense actin structures
285 exclude microtubules in epithelial cells *in vivo*.

286 Unexpectedly, despite the remaining accumulation of filamentous actin, Lat A-
287 treatment allowed some microtubules to pass through the accumulated actin (Figure
288 5 E, F). This result suggests that the accumulated actin undergo low levels of
289 depolymerization, leading to a decrease in the total density following Lat A-treatment
290 to allow microtubules to penetrate through the filamentous actin mass. Alternatively, a
291 moderate reduction in the density of accumulated actin may have been caused by

Latrunculin A itself, as it was reported to depolymerize actin filaments by severing and sequestering monomers (Fujiwara et al., 2018). Furthermore, the localization of membrane-bound mCD8-GFP was partially restored in the apical region of CAP mutant cells after Latrunculin A treatment (Figure 5 E, F). The result shows that microtubule-mediated transport of membrane-bound compartments to the apical regions is recovered by Latrunculin A treatment. Taken together, these results show that CAP loss of function leads to stable and dense apical actin structures, which likely forms a barrier that sterically prevents microtubule penetration and effective microtubule-based transport.

Accumulation of apical actin affects localization of microtubule-actin crosslinking protein spectraplakin/Shot, involved in non-centrosomal microtubule organization

In many epithelial cells, microtubules are organized in a non-centrosomal array, with their minus-ends anchored at the apical cortex and their plus-ends extending basally (Bacallao et al., 1989; Bré et al., 1990; Clark et al., 1997). A central mechanism enabling this organization is the anchoring and stabilization of microtubule minus-ends at the apical cortex by Patronin, the *Drosophila* homolog of CAMSAP3, together with Shot (Short stop; *Drosophila* homolog of MACF1/ACF7 and DST/BPAG1), a spectraplakin that crosslinks microtubules to the actin cytoskeleton. Both Patronin and Shot show sharp apical localization in follicle cells (Khanal et al., 2016; Nashchekin et al., 2016).

Next, to determine how apical actin accumulation affects microtubule organization, we examined the localization of Patronin and Shot in CAP mutant follicle cells. We found that Patronin, a microtubule minus-end–stabilizing and anchoring protein, remained apically localized in mutant cells, although its intensity appeared increased compared to wild-type cells (Figure 6A–C'). In contrast, the microtubule–actin crosslinking protein Shot was enriched beneath the accumulated apical actin in CAP mutant cells, rather than showing the sharp apical localization observed in wild type (Figure 6D–F').

These results indicate that excess apical actin affects Patronin and Shot differently: whereas Patronin localization is largely maintained, Shot fails to localize properly to the apical cortex. Nevertheless, because Dynein, whose localization marks microtubule minus-ends, remain enriched in the apical region (Figure 4I–K), the overall apical–basal polarity of non-centrosomal microtubules in CAP mutant cells appears to be preserved.

Dense apical actin prevents normal microtubule organization and leads to nuclear mispositioning

Organization of the non-centrosomal microtubules is required for proper nuclear positioning in various cellular contexts such as in *Drosophila* follicular epithelium as well as in mammalian intestinal epithelial cells (Khanal et al., 2016; Muroyama et al., 2018; Nashchekin et al., 2016; Toya et al., 2016). Consequently, defects in nuclear

positioning provide an independent readout to confirm microtubule-related phenotypes. We found that in CAP mutant cells, nuclei were mispositioned toward the apical region compared to the basal positions of the neighboring control cells (Figure 7 A). Surprisingly, reintroducing wild-type CAP into CAP mutant cells did not restore nuclear positioning, despite successfully rescuing actin accumulation, as well as earlier described phenotypes: organization of non-centrosomal microtubules, microvilli formation, and cytoplasmic mCD8-GFP localization in stage 10 (Figure 7 B, C). Quantitative analysis confirmed that the distance of the nuclei from the basal membrane was significantly greater in CAP mutants as compared to the controls (Figure 7 C). Furthermore, the nuclear mispositioning appeared even more evident in the rescued cells (Figure 7 B, C), possibly due to their better survival. Additionally, we did not observe any significant difference in the cell height between the control, CAP mutant and CAP wildtype rescue, suggesting that the observed nuclear position phenotype is independent of the cell height (Supl Fig 4 A). It is important to note that while we quantified nuclear positioning during stages 9-10, positioning occurs earlier, during stages 6-9 of oogenesis (Szikora et al., 2013). Thus, we asked if the CAP mutant phenotypes are visible at earlier stages of the follicle development. Indeed, the loss of CAP led to actin accumulation and disrupted apical microtubule organization in follicle cells during both early (stage 7, Figure 7 D) and late (stage 10, Figure 7 E) stages of oogenesis. However, the reintroduction of wild-type CAP only rescued actin accumulation and microtubule organization at stage 10, not at stage 7 (Figure 7 F, G). Further analysis showed that the CAP rescue construct was only minimally expressed during stages 6-7 (Supl Fig 4 B) indicating that the nuclear mispositioning phenotype, which develops during the early stages of oogenesis, could not be rescued by CAP expression at later stages. In conclusion, these results underscore the temporal requirement of CAP-mediated actin dynamics for establishing non-centrosomal microtubule arrays during early oogenesis for ensuring correct nuclear positioning.

DISCUSSION

Coordination of apical actin and microtubules

Our findings demonstrate that CAP-mediated apical actin turnover is needed for correct organization of non-centrosomal microtubule arrays in *Drosophila* follicular epithelium. The loss of function of Cyclase-Associated Protein (CAP, capt in *Drosophila*) leads to impenetrable ectopic apical actin forming a barrier that in turn disrupts apical organization of non-centrosomal microtubule arrays. As organization of noncentrosomal microtubules are disrupted, CAP mutant cells show defects in nuclear positioning, Dynein-based apical cargo trafficking, and the formation of apical microvilli. Our results highlight the role of CAP-mediated apical actin filament turnover

in microtubule organization, and suggest that apical actin turnover plays an important role in cytoskeletal coordination of epithelial cells.

The coordination of apical actin and non-centrosomal microtubules has been earlier explored in the context of epithelial morphogenesis, focusing on the generation of actomyosin-mediated contractile and adhesive forces (Röper, 2020). Current literature describes microtubules as regulators of apical actomyosin pool and coordinating actomyosin-based forces during apical constriction (Booth et al., 2014b; Corrigall et al., 2007; Ko et al., 2019b; J.-Y. Lee & Harland, 2007). Additionally, both apical actin turnover and non-centrosomal microtubules have been recognized as important regulators of force balance in epithelial cells (Ikawa & Sugimura, 2018; Jodoin et al., 2015). How and whether actin turnover, microtubule organization and actomyosin-based contractility are co-orchestrated during epithelial morphogenesis requires further investigation.

It is well-known that actin filament architectures actively modulate microtubules *in vitro* and in cultured cells (Cheng et al., 2023; Gélin et al., 2023; Gupton & Waterman-Storer, 2006; Waterman-Storer & Salmon, 1997). Also, loss of profilin, actin-binding protein facilitating the assembly of actin monomers into pre-existing actin filaments, results in changes in microtubule organization in cells, and therefore has been suggested to regulate both actin and microtubules (Henty-Ridilla et al., 2017; Liu et al., 2022; Nejedla et al., 2016). However, it has been recently postulated that the microtubule phenotypes associated with profilin loss are likely to result from adaptive responses of microtubules to changes in the actin cytoskeleton architecture and not as direct effect of loss of the profilin (Cisterna et al., 2024).

One mechanism by which filamentous actin directly regulates microtubules is through steric exclusion, where dense actin architectures can obstruct microtubule plus-end growth or cause their disassembly (Colin et al., 2018). Likely, the observed dense and persistent apical actin acts as a physical barrier to microtubules in CAP mutant cells. Thus, by promoting actin filament turnover CAP regulates actin filament architecture and density and may indirectly affect microtubules organization. This is supported by the observation that prolonged Latrunculin A treatment “loosens” the accumulated actin in CAP mutant cells, allowing microtubules to pass through. The actin cytoskeleton is known to sterically prevent microtubules in sites where the two cytoskeletal components converge in crowded spaces, such as at the leading edge of migrating cells or in neural growth cones (Dogterom & Koenderink, 2018; Pimm & Henty-Ridilla, 2021). In addition to regulating microtubules at the cell periphery, dense actin filaments in the centrosome reduce the number of centrosomal microtubules (Farina et al*.,* 2019; Inoue et al*.,* 2019). This suggests that dynamic changes in actin filament densities can be regulated according to the needs of microtubule assembly.

Dense apical actin prevents normal organization on non-centrosomal microtubules and results in nuclear mispostioning

The nuclear positioning phenotype of CAP-mutant cells suggests that apical actin turnover during early oogenesis is important for organization of non-centrosomal microtubules. In actively dividing cells, microtubules are typically nucleated by the centrosome, whereas in postmitotic epithelial cells, microtubules are organized into non-centrosomal arrays (Muroyama & Lechler, 2017). The transition from centrosomal to non-centrosomal microtubules coincides with the termination of cell divisions. In the follicular epithelium, cells divide until stage 6 (Klusza & Deng, 2011), suggesting that transition to non-centrosomal microtubules occurs thereafter. In follicle cells, nuclear positioning appears to be temporally connected to the establishment of non-centrosomal microtubule arrays during stages 6-9. In CAP mutant cells with stabilized apical actin, nuclei are positioned more apically compared to wild-type cells. Correct nuclear positioning in follicle cells is determined by the growing plus-ends of apically anchored microtubules that exert force to push nuclei to the correct apical-basal position (Szikora et al., 2013). Thus, the nuclear positioning phenotype in CAP mutant cells is likely caused by disorganization of non-centrosomal microtubules. These findings suggest that apical actin turnover is critical for correct nuclear positioning at the time when non-centrosomal microtubule arrays are established.

Correct organization of non-centrosomal microtubules is dependent on cortical anchoring of microtubule-minus ends mediated by Patronin and Shot. In addition, both Patronin and Shot are required for ensuring correct nuclear positioning across various cell types, from the *Drosophila* follicular epithelium to mammalian intestinal cells (Khanal et al., 2016; Muroyama et al., 2018; Nashchekin et al., 2016; Toya et al., 2016). Normally, Shot and Patronin exhibit sharp apical localization. In CAP mutant cells, however, Shot is localized ectopically beneath the accumulated actin. Ectopic Shot localization in CAP mutant cells may be explained by the fact that Shot's ability to bind microtubule lattices and promote actin-microtubule crosslinking is enhanced by increased filamentous actin densities (Applewhite et al., 2010, 2013; Takács et al., 2017). It is thus possible that in CAP mutant cells, accumulated actin traps Shot to ectopic sites, where Shot crosslinks microtubules and actin further impairing cytoskeletal coordination. To conclude, we demonstrate that efficient apical actin turnover mediated by CAP is needed for correct organization of non-centrosomal microtubule arrays to promote correct nuclear positioning.

Relevance of our findings and similarities to other polarized cells

Our current study enhances the understanding of CAP-mediated actin turnover in non-centrosomal microtubule organization. One of the earliest phenotypes associated with CAP loss-of-function was a defect in *Drosophila* oocyte polarity (Baum et al., 2000). In *Drosophila*, oocyte polarity is established by non-centrosomal microtubule arrays, that transport polarity-determining mRNAs to the anterior and posterior ends (St Johnston, 2023). In CAP mutant oocytes, these mRNAs are mislocalized, suggesting a defect in microtubule polarity. However, the mechanism by which CAP contributes to microtubule-related phenotypes has been incompletely understood. Like follicle

459 cells, in oocytes transition from centrosomal to non-centrosomal microtubule array
460 establishment is critical for oocyte polarity. In CAP mutant oocytes, excessive actin
461 accumulates at the anterior end (Baum et al., 2000). Intriguingly, this is the cortical site
462 where non-centrosomal microtubule arrays are normally anchored via Shot and
463 Patronin (Nashchekin et al., 2016). Our results show that in follicle cells CAP-mediated
464 actin turnover is critical for proper localization of Shot. Whether CAP-mediated actin
465 turnover is also required for the microtubule minus targeting in oocytes remains to be
466 investigated.

467 CAP is well-established for promoting actin dynamics in heart and skeletal muscle
468 cells, as well as in neuronal cells. Its loss results in actin accumulation, which impairs
469 muscle development and contraction, and affects neuronal growth cones and dendritic
470 spines (Field et al., 2015; Heinze et al., 2022; Kepser et al., 2019; Kumar et al., 2016;
471 Peche et al., 2013; Schneider et al., 2021). Furthermore, the loss of CAP activity, along
472 with excessive actin accumulation, has been linked to diseases such as nemaline
473 myopathy and Alzheimer's disease (Gurunathan et al., 2022; Pelucchi et al., 2020).
474 Our results shows that disruption of actin turnover and excessive accumulation of actin
475 in CAP mutant follicle cells can disrupt microtubule organization and microtubule-
476 based transport. Interestingly, in both muscle and neuronal cells, microtubules are
477 organized in a non-centrosomal manner (Bugnard et al., 2005; Kapitein &
478 Hoogenraad, 2015; Stiess et al., 2010; Tassin et al., 1985). However, the impact of
479 actin accumulation on microtubules has not been extensively studied muscle cells. In
480 neuronal cells it is known that persistent cofilin-actin rods disrupt microtubules and
481 impair microtubule-based trafficking (Cichon et al., 2012; Medina et al., 2008;
482 Minamide et al., 2000). Therefore, future studies are needed to determine how
483 disruption of actin turnover affects non-centrosomal microtubule arrays in other cellular
484 contexts, further elucidating the intricate interplay between actin dynamics and
485 microtubule organization in cells.

486 MATERIALS AND METHODS

487 *Drosophila* stocks

488 All the fly lines used in this study were obtained from Bloomington *Drosophila* Stock
489 Center or shared as gifts from other research groups. *Drosophila* fly line CaptE539,
490 an allele of Act up or Capulet (described as CAP) encoding a nonsense mutation at
491 tryptophan 141 (described in (Benlali et al., 2000), BDSC 5944) was used to generate
492 CAP (Cyclase-associated protein) chimeric loss-of-function mutant clones. Mitotic
493 mutant clones in the follicular epithelium were generated using FLP/FRT systems,
494 hsFLP; TubGal80, FRT40A; TubP-Gal4, UAS-mCD8-GFP/ TM6B, Tb (MARCM 40,
495 Gifted by Pernille Rørth) and hsflp; UbimRFPnls FRT40/cyo. Used genetypes for
496 experiments are described in Table 2 and Supplementary Table 1.

497 CAP loss of function clones were rescued with UAS fly lines encoding for wildtype
498 CAP and specific point mutations that abolished different biochemical activities of CAP.

499 These UAS-CAP fly lines were generated in-house for this project (see Table 1). UAS-
500 Chic, encoding for profilin was kind gift from Lynn Cooley. Endosomal trafficking in
501 mutant clones was analysed by combining Rab11-EYFP (BDSC 62549) with
502 CaptE593. Localization of F-actin crosslinker α-actinin is visualized by combining
503 CaptE593 with α-actinin-GFP (BDSC 602268). Localization of AIP1 was analyzed
504 using AIP1- protein trap AIP1GFP (BDSC 50824). Combining CaptE593 and Ubi-
505 p63E.Patronin GFP (BDSC 55129) were used to analyze the localization of
506 microtubule minus-end binding protein Ppatronin. All fly stocks were maintained at
507 18°C and crossed at 25°C in a standard food medium.

508 **Generation of CAP domain mutants**

509 Site-directed mutagenesis of selected amino acids to alanins (Table 1) was performed
510 within the longer cDNA of CAPT-RB (RH0878) isoform. The parts corresponding to
511 CAPT-RA isoform from the mutated CAPT-RB (RH0878, FlyBase ID FBtr0100023)
512 isoform were cloned into the pUAST-attB vector. PCR was amplified using DNA
513 polymerase enzyme KAPA HiFi (ReadyMix x 2, #KK2601, KAPA Biosystems; 30-60
514 sec/kb) following the recommended protocol. Resulting plasmids were verified with
515 sequencing. The transgenic flies were generated by BestGene inc. *Drosophila* embryo
516 injection services.

517 **Generation of mutant clones**

518 For the generation of mutant clones, 2–4-day-old female flies were transferred to
519 empty food vials and given two heat shocks at 37°C for one hour with a 5-hour interval
520 between each heat shock. After the two heat shocks, flies were kept in dry yeast and
521 allowed to recover for 3 days at 25°C. For rescue experiments clones were generated
522 up to 9 days prior dissections, in order toto ensure the disappearance of endogenous
523 CAP. After the recovery ovaries were dissected from these flies. The flies were
524 transferred to a fresh food medium containing wet yeast overnight before the
525 dissection.

526 **Producing recombinant Capt protein**

527 D. melanogaster Capt protein was expressed using pCoofy18 expression plasmid (a
528 kind gift from Sabine Suppmann, Addgene plasmid #43975) in BL21(DE3) E. coli
529 (Sigma-Aldrich). Protein purification was carried out essentially as described in Kotila
530 et al. 2018. In brief, collected bacterial cells were lysed in 50 mM Tris-HCl, 150 mM
531 NaCl, 25 mM imidazole, pH 7.5 buffer containing protease inhibitors. Supernatant was
532 clarified by centrifugation and loaded to HisTrap FF crude prepacked column (GE
533 Healthcare). Bound protein was eluted with imidazole gradient. Fractions containing
534 Capt were pooled and dialyzed O/N at 4°C in the presence of 3C protease in 50 mM
535 Tris-HCl, 150 mM NaCl, 1 mM DTT, pH 8.0 to remove 10xHis fusion tag. Dialyzed Capt
536 protein was concentrated with Amicon Ultra-4 centrifugal filter (Merck) and loaded to
537 HiLoad 16/600 SD 200 pg (GE Healthcare) column equilibrated in 5 mM HEPES,
538 50 mM NaCl, 0.2 mM DTT, 0.01% NaN3, pH 8.0 buffer. Fractions containing Capt

539 protein were concentrated as described above and snap frozen at 5-10 mg/ml
540 concentration using liquid N2 and stored at -80°C.

541 **Generation of Capt antibody**

542 Ig fractions of Capt-immunized rabbit serum (Pineda Antibody Service) were purified
543 by affinity chromatography from resin-antigen-coated beads. 500 µL of fraction was
544 eluted from the beads with 5 mL 0.1 M glycine-HCl (pH 2.8). The specificity of the
545 collected fractions was determined with the western blot of fly lysates of wild type
546 (W1118) and captE593 lysates. Additionally, immunostaining with purified anti-Capt
547 antibody showed decreased intensity in CaptE593 clones relative to the control cells.

548 **Dissection and Immunostaining**

549 Ovaries were dissected in ice-cold PBS and fixed in 4% paraformaldehyde for 20 min.
550 For acetylated α-tubulin staining, the ovaries were dissected in room temperature PBS
551 and fixed in 8% paraformaldehyde for 10 min. For Dynein heavy chain (Dynein-HC)
552 and Shot staining, ovaries were dissected in cold PBS and fixed for 10 min using
553 cytoskeleton buffer without glutaraldehyde, with 10% sucrose, 8% paraformaldehyde
554 and 0.05% Triton-X, thereafter ovaries were washed once with PBS and quenched
555 with sodium borohydride (NaBH4) for 10 min. The egg chambers are permeabilized in
556 0.1% BSA in 0.5% PBST and blocked with blocking buffer 2.5% BSA in 0.5% PBST.
557 The primary and secondary antibodies were diluted in the blocking buffer, and the
558 samples were incubated overnight at 4°C and for 2 hours at room temperature
559 respectively.

560 Primary antibodies used were rabbit anti-Capt (1:400, generated in the lab), mouse
561 anti-acetylated αtubulin (1:100, Santa Cruz biotechnology 6-11B-1), rabbit anti-
562 αTubulin (1:50, Abcam Ab18251), mouse anti-βTubulin (1:50, DSHB E7), mouse anti-
563 Shot (1:25, DSHB mABRod1), mouse anti-Cnx99A (1:25, DSHB Cnx99A 6-2-1),
564 mouse anti-Golgin84 (1:25, DSHB Golgin84 12-1), mouse anti-DyneinHC (1:25,
565 DSHB 2C11-2), rabbit anti-Cad99C (1:2000, gift from Christian Dahmann lab;
566 Schlichting et al., 2005), mouse anti-profilin (1:25, DSHB chi 1J), Twinfilin (gift from
567 Tapio Heino; Wahlström et al., 2001), mouse anti-Ena (1:25, DSHB 5G2), rat anti-
568 Tropomyosin (1:25, DSHB BB5/37.1) and rabbit anti-Phospho-Myosin II (1:300, Cell
569 Signalling Technologies). Secondary antibodies, donkey anti-mouse Alexa 647 and
570 goat anti-rabbit Alexa 647 (from Thermofisher Scientific), were used in a 1:300 dilution.
571 1µg/mL DAPI and Phalloidin (1:300, from Thermofisher Scientific) for staining the
572 nucleus and F-actin, respectively.

573 **Transmission electron microscopy**

574 Ovaries were dissected in cold 0.1M phosphate buffer (pH 7.4) and fixed in 2.5%
575 glutaraldehyde (EM-grade) and 2% paraformaldehyde in 0.1M phosphate buffer for 1
576 hour at room temperature and then continued at 4°C overnight. Egg chambers were
577 then washed with cold phosphate buffer on ice and post-fixed with 1% osmium

578 tetroxide in phosphate buffer for 1 hour on ice, later washed with dH2O and stained
579 with 1% uranyl acetate in dH2O at 4°C in the dark for 1 hour. After post-fixation and
580 EMem block staining, egg chambers were dehydrated through a gradient of ethanol,
581 rinsed with propylene oxide and gradually embedded into TAAB Hard epoxy resin. 60-
582 nm thin sections were cut using an ultramicrotome (Leica EM Ultracut UC7, Leica
583 Mikrosysteme GmbH, Austria), collected on Pioloform-coated single slot Copper grids
584 and poststained with uranyl acetate and lead citrate. TEM imaging was done using
585 JEM-1400 (JEOL Ltd, Japan) equipped with an Orius SC 1000B bottom-mounted
586 CCD-camera (Gatan Inc., USA) at accelerating voltage of 80 kV and magnifications
587 ranging from 8000 × to 100,000 ×. During TEM imaging the CAP mutant cells in
588 chimeric tissue were identified based on the phenotypes correlating with the
589 immunostaining such as loss of ER and golgi as well as reduced microvilli and
590 perivitelline space.

591 **Confocal microscopy and image analysis**

592 Confocal images were acquired using Leica SP8 Upright microscope using 20x and
593 63x oil immersion objectives. Image processing and analysis were conducted using
594 ImageJ software. Fluorescence intensity in the apical region was calculated as the
595 average value of all pixels within the ROI spanning the apical subcellular region. Data
596 for the Line scan intensity plots for CAPE593 were acquired from line ROIs parallel to
597 the apicobasal axis from the cross-section of the follicle cells. The distance is adjusted
598 such that 0 in the x-axis of the graphs corresponds to 25% of the total F-actin intensity.
599 The signal intensities are normalised to the maximum of the control sample, and
600 maximum-minimum normalisation was performed for the mean value for plotting. For
601 quantifying the nuclear position, the distance between the center of the nucleus to the
602 basal surface (in μm) is measured as a proxy to show the shift in the position of the
603 nucleus.

604 **Statistical analysis**

605 The outcomes were derived from a minimum of two autonomous experiments,
606 employing multiple egg chambers for analysis with reproducibility. Before performing
607 the statistical analysis normality of the data set was analyzed using the W test or the
608 Shapiro-Wilk test. For the normally distributed data sets, parametric tests, paired t-
609 tests were used and for non-parametric data sets, Mann-Whitney tests were used to
610 assess the significance of differences between the control and the CAPE593. For data
611 with more than two groups Kruskal-Wallis H test or one-way ANOVA was conducted.
612 The analysis was performed using OriginPro 2025 software.

613 **ACKNOWLEDGEMENTS**

614 We thank Lappalainen lab for helpful discussions during this work, and V. Hietakangas
615 and P. Lappalainen for critical reading providing feedback on the manuscript. We thank
616 A. Aalto, A. Haapalainen, J. Koivula, A. Poukova, P. Puonti, S. Rytövuori, and M.
617 Tolonen for excellent technical assistance. We thank Bloomington *Drosophila* Stock

Center, V. Hietakangas, P. Rorth, F. Besse and L. Cooley for providing fly stocks. We thank Developmental studies Hybridoma bank, C. Dahmann and T. Heino for providing antibodies. This study was facilitated by the University of Helsinki *Drosophila* core facility (Hi-Fly) and Institute of Biotechnology Light Microscopy Unit (LMU), Electron Microscopy Unit (EMBI), and Biomedicum Imaging Unit (BIU) of the University of Helsinki, supported by HiLIFE and Biocenter Finland.

Funding: This work is supported by grants from Academy of Finland (research fellowship 295549 and 137530 to M.P. and J.M, respectively) Sigrid Juselius Foundation (M.P. and J.M.), and Erkko Foundation (J.M.).

Author contributions: M.P. conceptualization. M.P. and A.B. experimental design. A.B. carried out majority of the experiments, validated and analyzed the data. S.M made some of the initial discoveries and performed the CAP mutant rescue experiments. K.K. and T.K. contributed to cloning and protein purification for antibody generation. V.H. and J.M. provided reagents and expertise. V.H., J.M. and M.P Supervision. A.B. and M.P. wrote the manuscript with input from all authors.

References

Applewhite, D. A., Grode, K. D., Duncan, M. C., & Rogers, S. L. (2013). The actin-microtubule cross-linking activity of *Drosophila* Short stop is regulated by intramolecular inhibition. *Molecular Biology of the Cell*, *24*(18), 2885–2893. https://doi.org/10.1091/mbc.e12-11-0798

Applewhite, D. A., Grode, K. D., Keller, D., Zadeh, A., Slep, K. C., & Rogers, S. L. (2010). The spectraplakin short stop is an actin-microtubule cross-linker that contributes to organization of the microtubule network. *Molecular Biology of the Cell*, *21*(10). https://doi.org/10.1091/mbc.E10-01-0011

Ballestrem, C., Wehrle-Haller, B., Hinz, B., & Imhof, B. A. (2000). Actin-dependent lamellipodia formation and microtubule-dependent tail retraction control-directed cell migration. *Molecular Biology of the Cell*, *11*(9). https://doi.org/10.1091/mbc.11.9.2999

Bartolini, F., & Gundersen, G. G. (2006). Generation of noncentrosomal microtubule arrays. *Journal of Cell Science*, *119*(20). https://doi.org/10.1242/jcs.03227

Baum, B., Li, W., & Perrimon, N. (2000). A cyclase-associated protein regulates actin and cell polarity during Drosophila oogenesis and in yeast. *Current Biology*, *10*(16). https://doi.org/10.1016/S0960-9822(00)00640-0

Baum, B., & Perrimon, N. (2001). Spatial control of the actin cytoskeleton in Drosophila epithelial cells. *Nature Cell Biology*, *3*(10). https://doi.org/10.1038/ncb1001-883

Benlali, A., Draskovic, I., Hazelett, D. J., & Treisman, J. E. (2000). Act up controls actin polymerization to alter cell shape and restrict Hedgehog signaling in the Drosophila eye disc. *Cell*, *101*(3). https://doi.org/10.1016/S0092-8674(00)80837-5

Bertling, E., Hotulainen, P., Mattila, P. K., Matilainen, T., Salminen, M., & Lappalainen, P. (2004). Cyclase-associated Protein 1 (CAP1) Promotes Cofilin-induced Actin Dynamics in Mammalian Nonmuscle Cells. *Molecular Biology of the Cell*, *15*(5). https://doi.org/10.1091/mbc.E04-01-0048

Bertling, E., Quintero-Monzon, O., Mattila, P. K., Goode, B. L., & Lappalaines, P. (2007). Mechanism and biological role of profilin-Srv2/CAP interaction. *Journal of Cell Science*, *120*(7). https://doi.org/10.1242/jcs.000158

Blanc, D., Bron, C., Gabert, J., Letourneur, F., MacDonald, H. R., & Malissen, B. (1988). Gene transfer of the ly-3 chain gene of the mouse cd8 molecular complex: co-transfer with the ly-2 polypeptide gene results in detectable cell surface expression of the ly-3 antigenic determinants. *European Journal of Immunology*, *18*(4). https://doi.org/10.1002/eji.1830180419

Booth, A. J. R., Blanchard, G. B., Adams, R. J., & Röper, K. (2014a). A Dynamic Microtubule Cytoskeleton Directs Medial Actomyosin Function during Tube Formation. *Developmental Cell*, *29*(5), 562–576. https://doi.org/10.1016/j.devcel.2014.03.023

Booth, A. J. R., Blanchard, G. B., Adams, R. J., & Röper, K. (2014b). A Dynamic microtubule cytoskeleton directs medial actomyosin function during tube formation. *Developmental Cell*, *29*(5). https://doi.org/10.1016/j.devcel.2014.03.023

Buckley, C. E., & St Johnston, D. (2022). Apical–basal polarity and the control of epithelial form and function. In *Nature Reviews Molecular Cell Biology* (Vol. 23, Number 8). https://doi.org/10.1038/s41580-022-00465-y

Bugnard, E., Zaal, K. J. M., & Ralston, E. (2005). Reorganization of microtubule nucleation during muscle differentiation. *Cell Motility and the Cytoskeleton*, *60*(1). https://doi.org/10.1002/cm.20042

Burr, A. A., Tsou, W. L., Ristic, G., & Todi, S. V. (2014). Using membrane-targeted green fluorescent protein to monitor neurotoxic protein-dependent degeneration of Drosophila eyes. *Journal of Neuroscience Research*, *92*(9). https://doi.org/10.1002/jnr.23395

Casanova, J. E., Wang, X., Kumar, R., Bhartur, S. G., Navarre, J., Woodrum, J. E., Altschuler, Y., Ray, G. S., & Goldenring, J. R. (1999). Association of Rab25 and Rab11a with the apical recycling system of polarized Madin-Darby Canine Kidney cells. *Molecular Biology of the Cell*, *10*(1). https://doi.org/10.1091/mbc.10.1.47

Chaudhry, F., Breitsprecher, D., Little, K., Sharov, G., Sokolova, O., & Goode, B. L. (2013). Srv2/cyclase-associated protein forms hexameric shurikens that directly catalyze actin filament severing by cofilin. *Molecular Biology of the Cell*, *24*(1). https://doi.org/10.1091/mbc.E12-08-0589

Cheng, H., Kao, Y., Chen, T., Sharma, L., Yang, W., Chuang, Y., Huang, S., Lin, H., Huang, Y., Kao, C., Yang, L., Bearon, R., Cheng, H., Hsia, K., & Lin, Y. (2023). Actin filaments form a size-dependent diffusion barrier around centrosomes. *EMBO Reports*, *24*(1). https://doi.org/10.15252/embr.202254935

Cichon, J., Sun, C., Chen, B., Jiang, M., Chen, X. A., Sun, Y., Wang, Y., & Chen, G. (2012). Cofilin aggregation blocks intracellular trafficking and induces synaptic loss in hippocampal neurons. *Journal of Biological Chemistry*, *287*(6). https://doi.org/10.1074/jbc.M111.301911

Cisterna, B. A., Skruber, K., Jane, M. L., Camesi, C. I., Nguyen, I. D., Liu, T. M., Warp, P. V., Black, J. B., Butler, M. T., Bear, J. E., Mor, D. E., Read, T. A., & Vitriol, E. A. (2024). Prolonged depletion of profilin 1 or F-actin causes an adaptive response in microtubules. *Journal of Cell Biology*, *223*(7). https://doi.org/10.1083/JCB.202309097/276742

Colin, A., Singaravelu, P., Théry, M., Blanchoin, L., & Gueroui, Z. (2018). Actin-Network Architecture Regulates Microtubule Dynamics. *Current Biology*, *28*(16). https://doi.org/10.1016/j.cub.2018.06.028

Corrigall, D., Walther, R. F., Rodriguez, L., Fichelson, P., & Pichaud, F. (2007). Hedgehog Signaling Is a Principal Inducer of Myosin-II-Driven Cell Ingression in Drosophila Epithelia. *Developmental Cell*, *13*(5), 730–742. https://doi.org/10.1016/j.devcel.2007.09.015

D'Alterio, C., Tran, D. D. D., Au Yeung, M. W. Y., Hwang, M. S. H., Li, M. A., Arana, C. J., Mulligan, V. K., Kubesh, M., Sharma, P., Chase, M., Tepass, U., & Godt, D. (2005). Drosophila melanogaster Cad99C, the orthologue of human Usher cadherin PCDH15, regulates the length of microvilli. *Journal of Cell Biology*, *171*(3). https://doi.org/10.1083/jcb.200507072

Dogterom, M., & Koenderink, G. H. (2018). Actin–microtubule crosstalk in cell biology. *Nature Reviews Molecular Cell Biology 2018 20:1*, *20*(1), 38–54. https://doi.org/10.1038/s41580-018-0067-1

Dogterom, M., & Koenderink, G. H. (2019). Actin–microtubule crosstalk in cell biology. In *Nature Reviews Molecular Cell Biology* (Vol. 20, Number 1). https://doi.org/10.1038/s41580-018-0067-1

Farina, F., Ramkumar, N., Brown, L., Samandar Eweis, D., Anstatt, J., Waring, T., Bithell, J., Scita, G., Thery, M., Blanchoin, L., Zech, T., & Baum, B. (2019). Local actin nucleation tunes centrosomal microtubule nucleation during passage

through mitosis. *The EMBO Journal*, *38*(11). https://doi.org/10.15252/embj.201899843

Field, J., Ye, D. Z., Shinde, M., Liu, F., Schillinger, K. J., Lu, M., Wang, T., Skettini, M., Xiong, Y., Brice, A. K., Chung, D. C., & Patel, V. V. (2015). CAP2 in cardiac conduction, sudden cardiac death and eye development. *Scientific Reports*, *5*. https://doi.org/10.1038/srep17256

Freeman, N. L., Chen, Z., Horenstein, J., Weber, A., & Field, J. (1995). An actin monomer binding activity localizes to the carboxyl-terminal half of the Saccharomyces cerevisiae cyclase-associated protein. *Journal of Biological Chemistry*, *270*(10). https://doi.org/10.1074/jbc.270.10.5680

Fujiwara, I., Zweifel, M. E., Courtemanche, N., & Pollard, T. D. (2018). Latrunculin A Accelerates Actin Filament Depolymerization in Addition to Sequestering Actin Monomers. *Current Biology*, *28*(19). https://doi.org/10.1016/j.cub.2018.07.082

Gélin, M., Schaeffer, A., Gaillard, J., Guérin, C., Vianay, B., Orhant-Prioux, M., Braun, M., Leterrier, C., Blanchoin, L., & Théry, M. (2023). Microtubules under mechanical pressure can breach dense actin networks. *Journal of Cell Science*, *136*(22). https://doi.org/10.1242/jcs.261667

Goodwin, S. S., & Vale, R. D. (2010). Patronin Regulates the Microtubule Network by Protecting Microtubule Minus Ends. *Cell*, *143*(2). https://doi.org/10.1016/j.cell.2010.09.022

Gupton, S. L., Salmon, W. C., & Waterman-Storer, C. M. (2002). Converging populations of f-actin promote breakage of associated microtubules to spatially regulate microtubule turnover in migrating cells. *Current Biology*, *12*(22). https://doi.org/10.1016/S0960-9822(02)01276-9

Gupton, S. L., & Waterman-Storer, C. M. (2006). Spatiotemporal Feedback between Actomyosin and Focal-Adhesion Systems Optimizes Rapid Cell Migration. *Cell*, *125*(7). https://doi.org/10.1016/j.cell.2006.05.029

Gurunathan, S., Sebastian, J., Baker, J., Abdel-Hamid, H. Z., West, S. C., Feingold, B., Peche, V., Reyes-Múgica, M., Madan-Khetarpal, S., & Field, J. (2022). A homozygous CAP2 pathogenic variant in a neonate presenting with rapidly progressive cardiomyopathy and nemaline rods. *American Journal of Medical Genetics, Part A*, *188*(3). https://doi.org/10.1002/ajmg.a.62590

Gutzeit, H. (1986). The role of microtubules in the differentiation of ovarian follicles during vitellogenesis inDrosophila. *Roux's Archives of Developmental Biology*, *195*(3), 173–181. https://doi.org/10.1007/BF02439435

Harris, T. J. C., & Peifer, M. (2005). The positioning and segregation of apical cues during epithelial polarity establishment in Drosophila. *Journal of Cell Biology*, *170*(5). https://doi.org/10.1083/jcb.200505127

Heinze, A., Schuldt, C., Khudayberdiev, S., van Bommel, B., Hacker, D., Schulz, T. G., Stringhi, R., Marcello, E., Mikhaylova, M., & Rust, M. B. (2022). Functional interdependence of the actin regulators CAP1 and cofilin1 in control of dendritic spine morphology. *Cellular and Molecular Life Sciences*, *79*(11). https://doi.org/10.1007/s00018-022-04593-8

Henty-Ridilla, J. L., Juanes, M. A., & Goode, B. L. (2017). Profilin Directly Promotes Microtubule Growth through Residues Mutated in Amyotrophic Lateral Sclerosis. *Current Biology*, *27*(22). https://doi.org/10.1016/j.cub.2017.10.002

Horne-Badovinac, S., & Bilder, D. (2008). Dynein regulates epithelial polarity and the apical localization of stardust A mRNA. *PLoS Genetics*, *4*(1). https://doi.org/10.1371/journal.pgen.0040008

Ikawa, K., & Sugimura, K. (2018). AIP1 and cofilin ensure a resistance to tissue tension and promote directional cell rearrangement. *Nature Communications*, *9*(1). https://doi.org/10.1038/s41467-018-05605-7

Inoue, D., Obino, D., Pineau, J., Farina, F., Gaillard, J., Guerin, C., Blanchoin, L., Lennon-Duménil, A., & Théry, M. (2019). Actin filaments regulate microtubule growth at the centrosome. *The EMBO Journal*, *38*(11). https://doi.org/10.15252/embj.201899630

Jansen, S., Collins, A., Golden, L., Sokolova, O., & Goode, B. L. (2014). Structure and mechanism of mouse cyclase-associated protein (CAP1) in regulating actin dynamics. *Journal of Biological Chemistry*, *289*(44). https://doi.org/10.1074/jbc.M114.601765

Jing, J., & Prekeris, R. (2009). Polarized endocytic transport: The roles of rab11 and rab11-FIPs in regulating cell polarity. In *Histology and Histopathology* (Vol. 24, Number 9).

Jodoin, J. N., Coravos, J. S., Chanet, S., Vasquez, C. G., Tworoger, M., Kingston, E. R., Perkins, L. A., Perrimon, N., & Martin, A. C. (2015). Stable Force Balance between Epithelial Cells Arises from F-Actin Turnover. *Developmental Cell*, *35*(6), 685–697. https://doi.org/10.1016/J.DEVCEL.2015.11.018

Kapitein, L. C., & Hoogenraad, C. C. (2015). Building the Neuronal Microtubule Cytoskeleton. In *Neuron* (Vol. 87, Number 3). https://doi.org/10.1016/j.neuron.2015.05.046

Kepser, L. J., Damar, F., De Cicco, T., Chaponnier, C., Prószynski, T. J., Pagenstecher, A., & Rust, M. B. (2019). CAP2 deficiency delays myofibril actin cytoskeleton differentiation and disturbs skeletal muscle architecture and function. *Proceedings of the National Academy of Sciences of the United States of America*, *116*(17). https://doi.org/10.1073/pnas.1813351116

Khanal, I., Elbediwy, A., de la Loza, M. del C. D., Fletcher, G. C., & Thompson, B. J. (2016). Shot and Patronin polarise microtubules to direct membrane traffic and biogenesis of microvilli in epithelia. *Journal of Cell Science*, *129*(13). https://doi.org/10.1242/jcs.189076

Klusza, S., & Deng, W. (2011). At the crossroads of differentiation and proliferation: Precise control of cell-cycle changes by multiple signaling pathways in *Drosophila* follicle cells. *BioEssays*, *33*(2), 124–134. https://doi.org/10.1002/bies.201000089

Knowles, B. C., Roland, J. T., Krishnan, M., Tyska, M. J., Lapierre, L. A., Dickman, P. S., Goldenring, J. R., & Shub, M. D. (2014). Myosin Vb uncoupling from RAB8A and RAB11A elicits microvillus inclusion disease. *Journal of Clinical Investigation*, *124*(7). https://doi.org/10.1172/JCI71651

Ko, C. S., Tserunyan, V., & Martin, A. C. (2019a). Microtubules promote intercellular contractile force transmission during tissue folding. *Journal of Cell Biology*, *218*(8), 2726–2742. https://doi.org/10.1083/jcb.201902011

Ko, C. S., Tserunyan, V., & Martin, A. C. (2019b). Microtubules promote intercellular contractile force transmission during tissue folding. *Journal of Cell Biology*, *218*(8), 2726–2742. https://doi.org/10.1083/jcb.201902011

Kotila, T., Kogan, K., Enkavi, G., Guo, S., Vattulainen, I., Goode, B. L., & Lappalainen, P. (2018). Structural basis of actin monomer re-charging by cyclase-Associated protein. *Nature Communications*, *9*(1). https://doi.org/10.1038/s41467-018-04231-7

Kotila, T., Wioland, H., Enkavi, G., Kogan, K., Vattulainen, I., Jégou, A., Romet-Lemonne, G., & Lappalainen, P. (2019). Mechanism of synergistic actin filament pointed end depolymerization by cyclase-associated protein and cofilin. *Nature Communications*, *10*(1). https://doi.org/10.1038/s41467-019-13213-2

Kreitzer, G., & Myat, M. M. (2018). Microtubule motors in establishment of epithelial cell polarity. *Cold Spring Harbor Perspectives in Biology*, *10*(2). https://doi.org/10.1101/cshperspect.a027896

Kumar, A., Paeger, L., Kosmas, K., Kloppenburg, P., Noegel, A. A., & Peche, V. S. (2016). Neuronal actin dynamics, spine density and neuronal dendritic complexity are regulated by CAP2. *Frontiers in Cellular Neuroscience*, *10*. https://doi.org/10.3389/fncel.2016.00180

Lappalainen, P., Kotila, T., Jégou, A., & Romet-Lemonne, G. (2022). Biochemical and mechanical regulation of actin dynamics. In *Nature Reviews Molecular Cell Biology* (Vol. 23, Number 12). https://doi.org/10.1038/s41580-022-00508-4

Lee, J.-Y., & Harland, R. M. (2007). Actomyosin contractility and microtubules drive apical constriction in Xenopus bottle cells. *Developmental Biology*, *311*(1), 40–52. https://doi.org/10.1016/j.ydbio.2007.08.010

Lee, S., & Kolodziej, P. A. (2002). Short stop provides an essential link between F-actin and microtubules during axon extension. *Development*, *129*(5). https://doi.org/10.1242/dev.129.5.1195

Lee, T., & Luo, L. (2001). Mosaic analysis with a repressible cell marker (MARCM) for Drosophila neural development. *Trends in Neurosciences*, *24*(5), 251–254. https://doi.org/10.1016/S0166-2236(00)01791-4

Lila, T., & Drubin, D. G. (1997). Evidence for physical and functional interactions among two Saccharomyces cerevisiae SH3 domain proteins, an adenylyl cyclase-associated protein and the actin cytoskeleton. *Molecular Biology of the Cell*, *8*(2). https://doi.org/10.1091/mbc.8.2.367

Liu, X., Pimm, M. L., Haarer, B., Brawner, A. T., & Henty-Ridilla, J. L. (2022). Biochemical characterization of actin assembly mechanisms with ALS-associated profilin variants. *European Journal of Cell Biology*, *101*(2). https://doi.org/10.1016/j.ejcb.2022.151212

Martin, A. C., Kaschube, M., & Wieschaus, E. F. (2009). Pulsed contractions of an actin-myosin network drive apical constriction. *Nature*, *457*(7228). https://doi.org/10.1038/nature07522

Mattila, P. K., Quintero-Monzon, O., Kugler, J., Moseley, J. B., Almo, S. C., Lappalainen, P., & Goode, B. L. (2004). A high-affinity interaction with ADP-actin monomers underlies the mechanism and in vivo function of Srv2/cyclase-associated protein. *Molecular Biology of the Cell*, *15*(11). https://doi.org/10.1091/mbc.E04-06-0444

Meads, T., & Schroer, T. A. (1995). Polarity and nucleation of microtubules in polarized epithelial cells. *Cell Motility and the Cytoskeleton*, *32*(4). https://doi.org/10.1002/cm.970320404

Medina, P. M. B., Worthen, R. J., Forsberg, L. J., & Brenman, J. E. (2008). The actin-binding protein capulet genetically interacts with the microtubule motor kinesin to maintain neuronal dendrite homeostasis. *PLoS ONE*, *3*(8). https://doi.org/10.1371/journal.pone.0003054

Meiring, J. C. M., Shneyer, B. I., & Akhmanova, A. (2020). Generation and regulation of microtubule network asymmetry to drive cell polarity. In *Current Opinion in Cell Biology* (Vol. 62). https://doi.org/10.1016/j.ceb.2019.10.004

Minamide, L. S., Striegl, A. M., Boyle, J. A., Meberg, P. J., & Bamburg, J. R. (2000). Neurodegenerative stimuli induce persistent ADF/cofilin-actin rods that

disrupt distal neurite function. *Nature Cell Biology*, *2*(9). https://doi.org/10.1038/35023579

Mogensen, M. M., & Tucker, J. B. (1987). Evidence for microtubule nucleation at plasma membrane-associated sites in Drosophila. *Journal of Cell Science*, *88 (Pt 1)*. https://doi.org/10.1242/jcs.88.1.95

Moriyama, K., & Yahara, I. (2002). Human CAP1 is a key factor in the recycling of cofilin and actin for rapid actin turnover. *Journal of Cell Science*, *115*(8). https://doi.org/10.1242/jcs.115.8.1591

Muroyama, A., & Lechler, T. (2017). Microtubule organization, dynamics and functions in differentiated cells. *Development*, *144*(17), 3012–3021. https://doi.org/10.1242/dev.153171

Muroyama, A., Terwilliger, M., Dong, B., Suh, H., & Lechler, T. (2018). Genetically induced microtubule disruption in the mouse intestine impairs intracellular organization and transport. *Molecular Biology of the Cell*, *29*(13). https://doi.org/10.1091/mbc.E18-01-0057

Nashchekin, D., Fernandes, A. R., & St Johnston, D. (2016). Patronin/Shot Cortical Foci Assemble the Noncentrosomal Microtubule Array that Specifies the Drosophila Anterior-Posterior Axis. *Developmental Cell*, *38*(1). https://doi.org/10.1016/j.devcel.2016.06.010

Nejedla, M., Sadi, S., Sulimenko, V., De Almeida, F. N., Blom, H., Draber, P., Aspenström, P., & Karlsson, R. (2016). Profilin connects actin assembly with microtubule dynamics. *Molecular Biology of the Cell*, *27*(15). https://doi.org/10.1091/mbc.E15-11-0799

Ning, W., Yu, Y., Xu, H., Liu, X., Wang, D., Wang, J., Wang, Y., & Meng, W. (2016). The CAMSAP3-ACF7 Complex Couples Noncentrosomal Microtubules with Actin Filaments to Coordinate Their Dynamics. *Developmental Cell*, *39*(1). https://doi.org/10.1016/j.devcel.2016.09.003

Noordstra, I., Liu, Q., Nijenhuis, W., Hua, S., Jiang, K., Baars, M., Remmelzwaal, S., Martin, M., Kapitein, L. C., & Akhmanova, A. (2016). Control of apico-basal epithelial polarity by the microtubule minus-end-binding protein CAMSAP3 and spectraplakin ACF7. *Journal of Cell Science*, *129*(22). https://doi.org/10.1242/jcs.194878

Ono, S. (2013). The role of cyclase-associated protein in regulating actin filament dynamics - more than a monomer-sequestration factor. In *Journal of Cell Science* (Vol. 126, Number 15). https://doi.org/10.1242/jcs.128231

Peche, V. S., Holak, T. A., Burgute, B. D., Kosmas, K., Kale, S. P., Wunderlich, F. T., Elhamine, F., Stehle, R., Pfitzer, G., Nohroudi, K., Addicks, K., Stöckigt, F., Schrickel, J. W., Gallinger, J., Schleicher, M., & Noegel, A. A. (2013). Ablation of

cyclase-associated protein 2 (CAP2) leads to cardiomyopathy. *Cellular and Molecular Life Sciences*, *70*(3). https://doi.org/10.1007/s00018-012-1142-y

Pelaseyed, T., & Bretscher, A. (2018). Regulation of actin-based apical structures on epithelial cells. In *Journal of Cell Science* (Vol. 131, Number 20). https://doi.org/10.1242/jcs.221853

Pelucchi, S., Vandermeulen, L., Pizzamiglio, L., Aksan, B., Yan, J., Konietzny, A., Bonomi, E., Borroni, B., Padovani, A., Rust, M. B., Di Marino, D., Mikhaylova, M., Mauceri, D., Antonucci, F., Edefonti, V., Gardoni, F., Di Luca, M., & Marcello, E. (2020). Cyclase-associated protein 2 dimerization regulates cofilin in synaptic plasticity and Alzheimer's disease. *Brain Communications*, *2*(2). https://doi.org/10.1093/braincomms/fcaa086

Perrin, L., & Matic Vignjevic, D. (2023). The emerging roles of the cytoskeleton in intestinal epithelium homeostasis. In *Seminars in Cell and Developmental Biology* (Vols. 150–151). https://doi.org/10.1016/j.semcdb.2023.03.008

Pimm, M. L., & Henty-Ridilla, J. L. (2021). New twists in actin-microtubule interactions. *Molecular Biology of the Cell*, *32*(3), 211–217. https://doi.org/10.1091/MBC.E19-09-0491/ASSET/IMAGES/LARGE/MBC-32-211-G002.JPEG

Priya, R. (2022). Preprint Highlight: Dynamic interplay of protrusive microtubule and contractile actomyosin forces drive tissue extension. *Molecular Biology of the Cell*, *33*(12). https://doi.org/10.1091/mbc.p22-07-1012

Quintero-Monzon, O., Jonasson, E. M., Bertling, E., Talarico, L., Chaudhry, F., Sihvo, M., Lappalainen, P., & Goode, B. L. (2009). Reconstitution and Dissection of the 600-kDa Srv2/CAP Complex. *Journal of Biological Chemistry*, *284*(16), 10923–10934. https://doi.org/10.1074/JBC.M808760200

Raman, R., Pinto, C. S., & Sonawane, M. (2018). Polarized Organization of the Cytoskeleton: Regulation by Cell Polarity Proteins. In *Journal of Molecular Biology* (Vol. 430, Number 19). https://doi.org/10.1016/j.jmb.2018.06.028

Reck-Peterson, S. L., Redwine, W. B., Vale, R. D., & Carter, A. P. (2018). The cytoplasmic dynein transport machinery and its many cargoes. In *Nature Reviews Molecular Cell Biology* (Vol. 19, Number 6). https://doi.org/10.1038/s41580-018-0004-3

Ricolo, D., & Araújo, S. J. (2020). Coordinated crosstalk between microtubules and actin by a spectraplakin regulates lumen formation and branching. *ELife*, *9*. https://doi.org/10.7554/eLife.61111

Roeth, J. F., Sawyer, J. K., Wilner, D. A., & Peifer, M. (2009). Rab11 helps maintain apical crumbs and adherens junctions in the drosophila embryonic ectoderm. *PLoS ONE*, *4*(10). https://doi.org/10.1371/journal.pone.0007634

Roh-Johnson, M., Shemer, G., Higgins, C. D., McClellan, J. H., Werts, A. D., Tulu, U. S., Gao, L., Betzig, E., Kiehart, D. P., & Goldstein, B. (2012). Triggering a cell shape change by exploiting preexisting actomyosin contractions. *Science*, *335*(6073). https://doi.org/10.1126/science.1217869

Röper, K. (2020). Microtubules enter centre stage for morphogenesis. In *Philosophical Transactions of the Royal Society B: Biological Sciences* (Vol. 375, Number 1809). https://doi.org/10.1098/rstb.2019.0557

Sauvanet, C., Wayt, J., Pelaseyed, T., & Bretscher, A. (2015). Structure, Regulation, and Functional Diversity of Microvilli on the Apical Domain of Epithelial Cells. *Annual Review of Cell and Developmental Biology*, *31*. https://doi.org/10.1146/annurev-cellbio-100814-125234

Schlichting, K., Demontis, F., & Dahmann, C. (2005). Cadherin Cad99C is regulated by Hedgehog signaling in Drosophila. *Developmental Biology*, *279*(1). https://doi.org/10.1016/j.ydbio.2004.12.008

Schneider, F., Duong, T. A., Metz, I., Winkelmeier, J., Hübner, C. A., Endesfelder, U., & Rust, M. B. (2021). Mutual functional dependence of cyclase-associated protein 1 (CAP1) and cofilin1 in neuronal actin dynamics and growth cone function. *Progress in Neurobiology*, *202*. https://doi.org/10.1016/j.pneurobio.2021.102050

Sharkova, M., Chow, E., Erickson, T., & Hocking, J. C. (2023). The morphological and functional diversity of apical microvilli. *Journal of Anatomy*, *242*(3), 327–353. https://doi.org/10.1111/joa.13781

Shekhar, S., Chung, J., Kondev, J., Gelles, J., & Goode, B. L. (2019). Synergy between Cyclase-associated protein and Cofilin accelerates actin filament depolymerization by two orders of magnitude. *Nature Communications*, *10*(1). https://doi.org/10.1038/s41467-019-13268-1

Singh, A., Saha, T., Begemann, I., Ricker, A., Nüsse, H., Thorn-Seshold, O., Klingauf, J., Galic, M., & Matis, M. (2018). Polarized microtubule dynamics directs cell mechanics and coordinates forces during epithelial morphogenesis. In *Nature Cell Biology* (Vol. 20, Number 10). https://doi.org/10.1038/s41556-018-0193-1

Singh, A., Thale, S., Leibner, T., Lamparter, L., Ricker, A., Nüsse, H., Klingauf, J., Galic, M., Ohlberger, M., & Matis, M. (2024). Dynamic interplay of microtubule and actomyosin forces drive tissue extension. *Nature Communications*, *15*(1), 3198. https://doi.org/10.1038/s41467-024-47596-8

Spector, I., Shochet, N. R., Kashman, Y., & Groweiss, A. (1983). Latrunculins: Novel marine toxins that disrupt microfilament organization in cultured cells. *Science*, *219*(4584). https://doi.org/10.1126/science.6681676

St Johnston, D. (2023). *Polarity and axis formation in the Drosophila female germ line* (pp. 73–97). https://doi.org/10.1016/bs.ctdb.2023.02.002

Stiess, M., Maghelli, N., Kapitein, L. C., Gomis-Rüth, S., Wilsch-Bräuninger, M., Hoogenraad, C. C., Tolić-Nørrelykke, I. M., & Bradke, F. (2010). Axon extension occurs independently of centrosomal microtubule nucleation. *Science*, *327*(5966). https://doi.org/10.1126/science.1182179

Szikora, S., Gaspar, I., & Szabad, J. (2013). “Poking” microtubules bring about nuclear wriggling to position nuclei. *Journal of Cell Science*, *126*(1). https://doi.org/10.1242/jcs.114355

Takács, Z., Jankovics, F., Vilmos, P., Lénárt, P., Röper, K., & Erdélyi, M. (2017). The spectraplakin Short stop is an essential microtubule regulator involved in epithelial closure in *Drosophila*. *Journal of Cell Science*, *130*(4), 712–724. https://doi.org/10.1242/jcs.193003

Tassin, A. M., Maro, B., & Bornens, M. (1985). Fate of microtubule-organizing centers during myogenesis in vitro. *Journal of Cell Biology*, *100*(1). https://doi.org/10.1083/jcb.100.1.35

Toya, M., Kobayashi, S., Kawasaki, M., Shioi, G., Kaneko, M., Ishiuchi, T., Misaki, K., Meng, W., & Takeichi, M. (2016). CAMSAP3 orients the apical-to-basal polarity of microtubule arrays in epithelial cells. *Proceedings of the National Academy of Sciences of the United States of America*, *113*(2). https://doi.org/10.1073/pnas.1520638113

Toya, M., & Takeichi, M. (2016). Organization of non-centrosomal microtubules in epithelial cells. *Cell Structure and Function*, *41*(2). https://doi.org/10.1247/csf.16015

Vojtek, A., Haarer, B., Field, J., Gerst, J., Pollard, T. D., Brown, S., & Wigler, M. (1991). Evidence for a functional link between profilin and CAP in the yeast S. cerevisiae. *Cell*, *66*(3). https://doi.org/10.1016/0092-8674(81)90013-1

Waterman-Storer, C. M., & Salmon, E. D. (1997). Actomyosin-based retrograde flow of microtubules in the lamella of migrating epithelial cells influences microtubule dynamic instability and turnover and is associated with microtubule breakage and treadmilling. *Journal of Cell Biology*, *139*(2). https://doi.org/10.1083/jcb.139.2.417

Wilkie, G. S., & Davis, I. (2001). Drosophila wingless and pair-rule transcripts localize apically by dynein-mediated transport of RNA particles. *Cell*, *105*(2). https://doi.org/10.1016/S0092-8674(01)00312-9

Zhou, J., Kim, H. Y., Wang, J. H. C., & Davidson, L. A. (2010). Macroscopic stiffening of embryonic tissues via microtubules, RhoGEF and the assembly of

contractile bundles of actomyosin. *Development*, *137*(16). https://doi.org/10.1242/dev.045997

1042 **Figure legends**

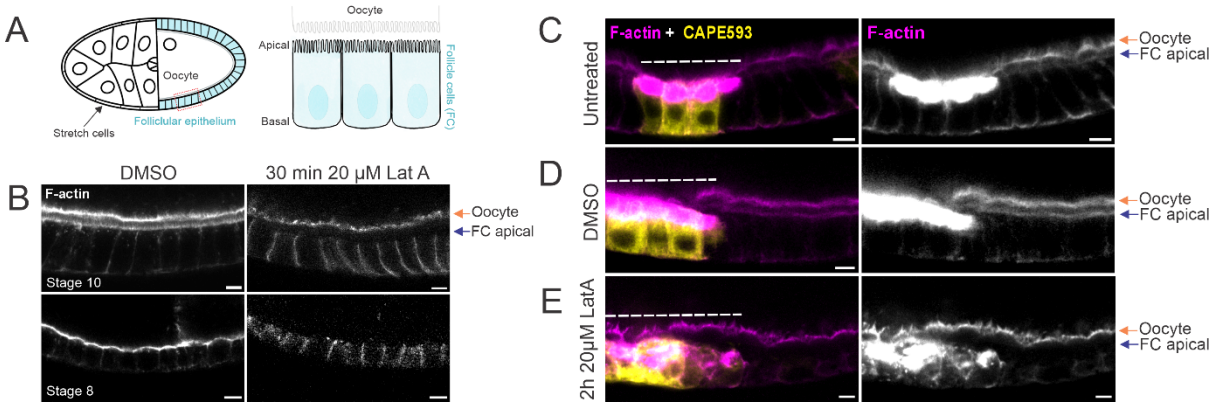

1043

1044 **Figure 1**: **Loss of CAP disrupts fast turnover of apical actin. (A) Illustration of stage 10**
1045 ***Drosophila* melanogaster egg chamber** highlighting the apicobasal polarization of the
1046 follicular epithelium. The black arrow points towards the squamous cells called stretch cells.
1047 **(B) Latrunculin A treatment reveals filamentous actin structures that are under fast**
1048 **turnover.** Treatment of egg chambers with DMSO (control) and 20 µM Latrunculin A for 30-
1049 minutes results in a decrease in filamentous actin structures under fast turnover. In stage 10
1050 follicular epithelium, filamentous actin (stained with Phalloidin) is decreased in apical microvilli,
1051 apical actin cortex, and basal stress fibres, while junctional actin and the oocyte actin cortex
1052 appear to be less affected. In stage 8 follicular epithelium, Latrunculin A induces depletion of
1053 both apical actin and basal actin in the follicle cells, while junctional actin remains unaffected.
1054 The orange arrow highlights the oocyte cortex, and the blue arrow highlights apical surface of
1055 the follicle cells. Scale bar = 10 µm. **(C) Loss of CAP results in apical actin accumulation.**
1056 Mosaic follicular epithelium with CAP mutant cells (GFP, pseudo-colored yellow, dotted line)
1057 exhibiting significant apical actin accumulation (Phalloidin, pseudo-colored magenta). Scale
1058 bar = 10 µm. **(D-E) Even prolonged Latrunculin A treatment failed to fully disassemble**
1059 **dense accumulated actin of CAP mutant cells.** Mosaic follicular epithelium with CAP mutant
1060 cells marked with mCD8-GFP (GFP positive, pseudo-colored yellow, dashed line), stained for
1061 filamentous actin (stained with phalloidin, pseudo-colored magenta) treated with DMSO
1062 (control) **(D)** and 20 µM Latrunculin A **(E)** for 2 hours. Upon treatment with Latrunculin A, apical
1063 actin accumulation persisted in CAP mutant cells whereas a decrease in apical F-actin was
1064 observed in the neighbouring control cells. Scale bar = 10 µm.

1065

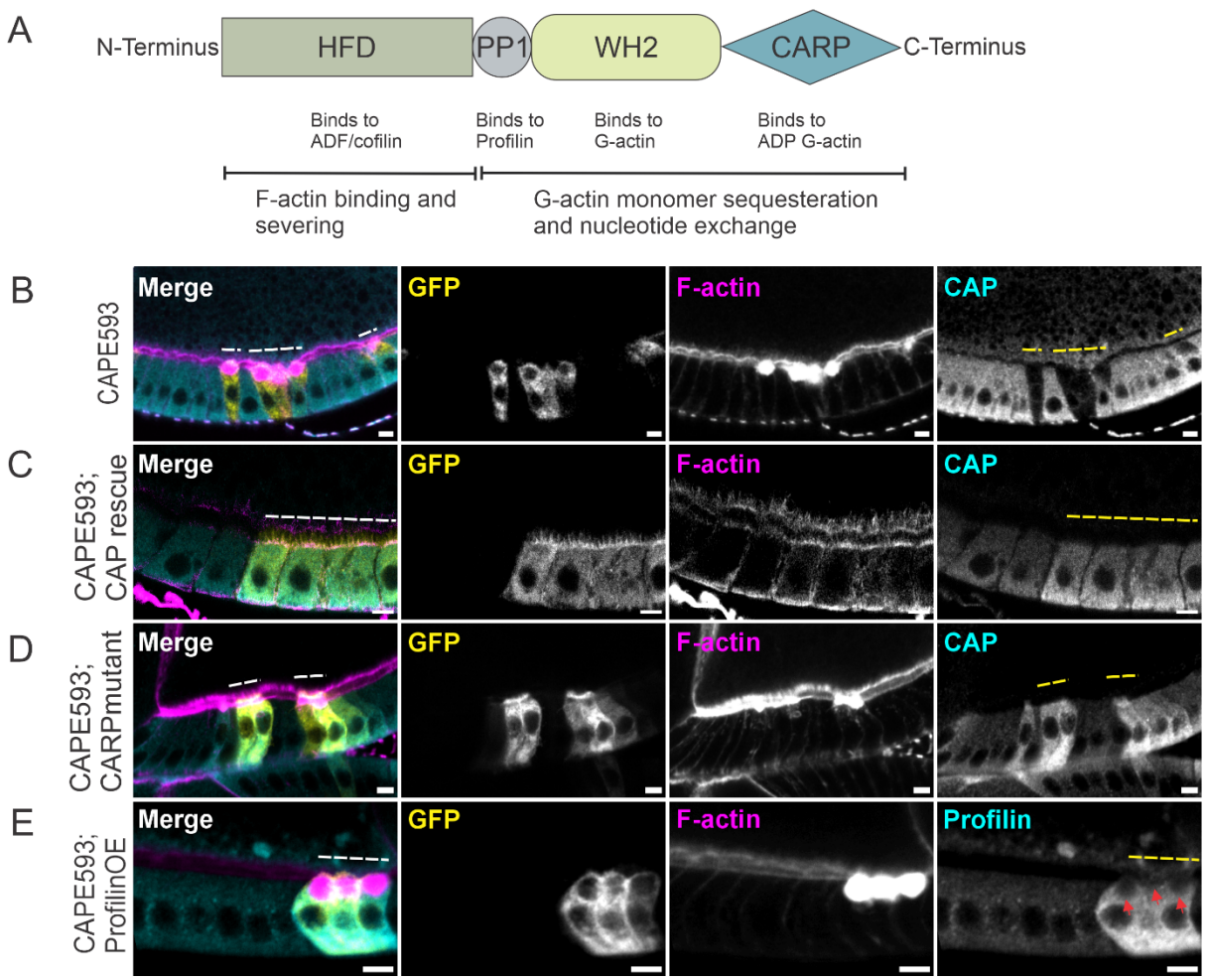

Figure 2. Nucleotide exchange activity of CAP is critical for apical actin turnover. (A) Schematic diagram of protein domain organization of CAP. (B) CAP mutant cells shows apical actin accumulation. Mosaic follicular epithelium with CAP mutant cells (GFP, pseudo-colored yellow, dashed line) exhibiting significant apical actin accumulation (Phalloidin, pseudo-colored magenta) alongside a loss of CAP expression (immunostaining, pseudo-colored cyan). Scale bar = 10 µm. **(C) CAP rescue restores apical actin accumulation.** Mosaic follicular epithelium with CAP mutant cells rescued with wildtype CAP (GFP positive, pseudo-colored yellow, dashed line) demonstrating restored apical actin accumulation (Phalloidin, pseudo-colored magenta) and expression of the CAP rescue construct (immunostaining, pseudo-colored cyan). Scale bar = 10 µm. **(D) CARP domain mutant fails to rescue apical actin accumulation.** Mosaic follicular epithelium with CAP mutant cells rescued with a CARP domain mutant of CAP (GFP positive, pseudo-colored yellow, dashed line) showing failure to restore apical actin accumulation (Phalloidin, pseudo-colored magenta). Expression of the CAP in CARP-domain rescue construct is depicted (immunostaining, pseudo-colored cyan). Scale bar = 10 µm. **(E) Profilin overexpression fails to rescue apical actin accumulation.** Mosaic follicular epithelium with CAP mutant cells overexpressing profilin (GFP positive, pseudo-colored yellow, dashed line) demonstrating failure to restore apical actin accumulation (Phalloidin, pseudo-colored magenta). The expression of the profilin construct is shown (immunostaining, pseudo-colored cyan). The

profilin expression is increased at the basal region of the cells. Red arrows denote the actin accumulation site lacking profilin localisation. Scale bar = 10 µm.

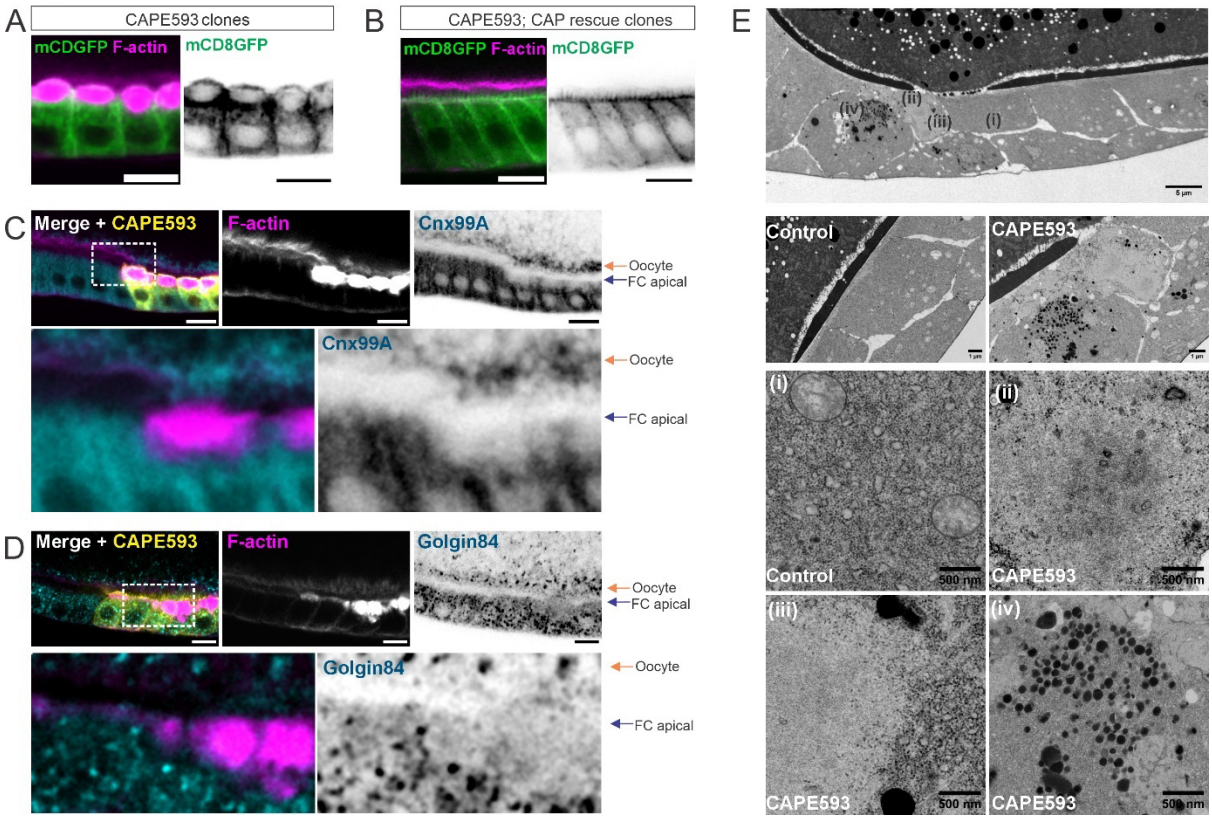

Figure 3. Membrane-bound organelles are excluded from site of actin accumulation (A) Absence of membrane-bound mCD8-GFP at site of actin accumulation in CAP mutant cells. Mosaic follicular epithelium with CAP mutant cells marked with mCD8-GFP (GFP positive, green) and filamentous actin (stained with phalloidin, pseudo-colored magenta). In CAP mutant cells, the membrane bound mCD8-GFP clonal marker (green) is absent in the region of actin accumulation (magenta). Scale bar = 10 µm. **(B) mCD8-GFP localization is restored upon CAP rescue. Mosaic follicular epithelium expressing wildtype CAP in CAP mutant cells.** CAP rescue (mCD8-GFP positive cells) restores the actin accumulation phenotype (F-actin, magenta) and re-establishes mCD8GFP (green) localization. Scale bar = 10 µm. **(C) The site of actin accumulation lacks ER markers.** Mosaic follicular epithelium with CAP mutant cells (GFP positive, pseudo-colored yellow) stained for F-actin (phalloidin, pseudo-colored magenta) and antibody against ER marker Calnexin99A (Cnx99A, pseudocoloured, cyan). Zoomed-in inset shows the apical region of the cell with a lack of ER markers at the site of F-actin accumulation. The orange arrow highlights the Cnx99A localisation on the oocyte cortex, and the blue arrow highlights the localisation of Cnx99A on the apical surface of the follicle cells (FC). Scale bar = 10 µm. **(D) The Golgi marker is lacking at the site of actin accumulation.** Mosaic follicular epithelium with CAP mutant cells (GFP positive, pseudo-colored yellow) stained for F-actin (phalloidin, pseudo-colored magenta) and antibody against Golgi marker Golgin84 (pseudocoloured, cyan). Zoomed-in inset shows the apical region of the cell with F-actin accumulation, lacking the Golgi marker Golgin84. The orange arrow highlights the Golgin84 localisation on the oocyte cortex, and the blue arrow highlights the localisation of Golgin84 on the apical surface of the follicle cells (FC). Scale bar

= 10 µm. **(E) Transmission electron microscopy (TEM) of CAP mutant cells.** Transmission electron microscopy (TEM) image of follicular epithelium with CAP mutant clones and control cells. The site of actin accumulation appears less dense than other regions of the cell and neighboring control cells and lacks organelles such as mitochondria, ER, and ribosomes. The numbered regions correspond to specified magnified insets. **(i)** Magnified region near the apical domain of the control cell, showing the presence of membrane-bound organelles like mitochondria. **(ii)** Magnified image of the region near the apical domain in CAP mutant cells, showing the lack of cytoplasmic components. **(iii)** Magnified image of the boundary of the site of actin accumulation, highlighting the difference in cytoplasmic components inside and outside of the accumulated actin. **(iv)** Magnified image showing the presence of electron-dense vesicular structures near the site of actin accumulation in CAP mutant cells.

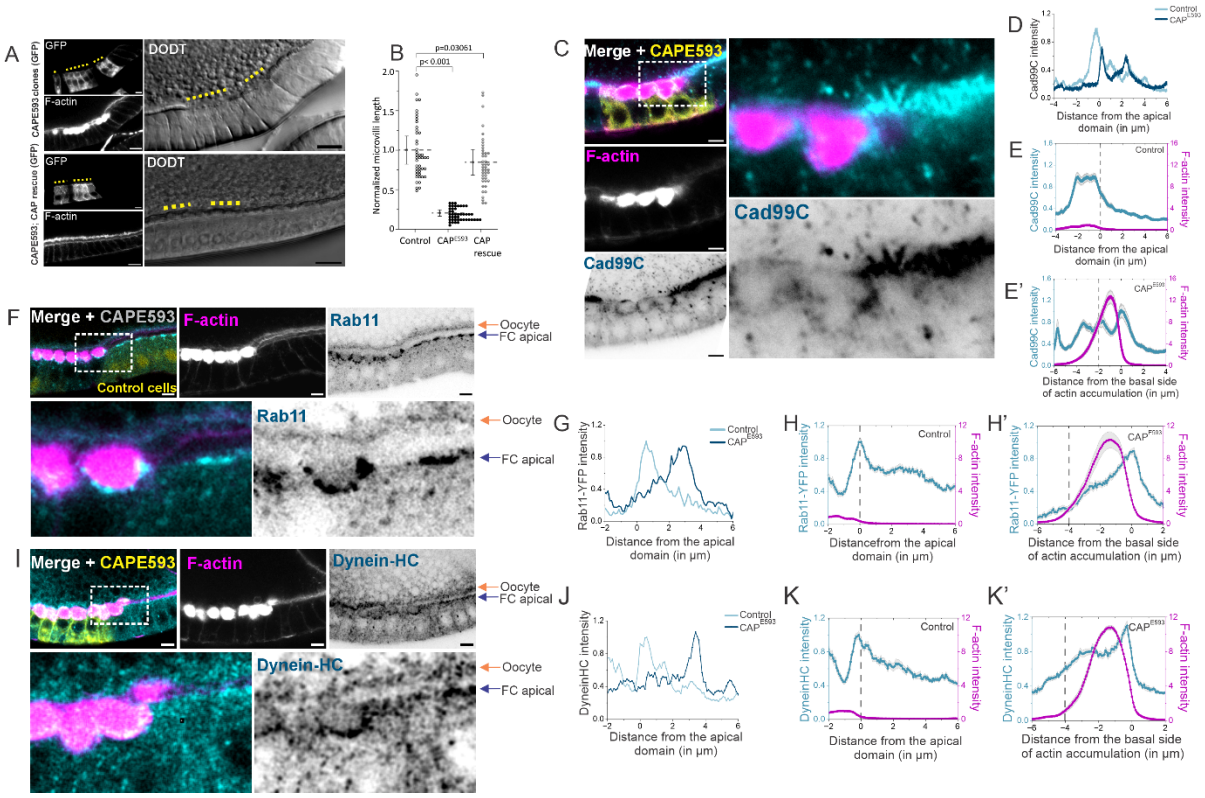

Figure 4. Apical actin accumulation halts Dynein and Rab11-mediated trafficking, leading to the retention of apical cargo Cad99C required for microvilli biogenesis. (A) Loss of apical microvilli in CAP mutant cells. Mosaic follicular epithelium with CAP mutant cells (GFP positive, dashed line). The gradient contrast (DODT) image shows the loss of apical microvilli in CAP mutant cells (dashed line). CAP mutant cells rescued with wild-type CAP expression (CAP rescue, GFP positive, dashed line) show the rescue of F-actin accumulation and apical microvilli. Scale bar = 10 µm. **(B) Quantification of microvilli length relative to control.** Quantification of microvilli length normalized with the control. The bar shows the ± 0.5 SD, and the dotted line represents the mean value. One-way ANOVA with post-hoc test was used to determine the statistical significance between different groups. Control = 45 cells, CAPE593 = 45 cells; CAP rescue = 43 cells. N = 9, 11, 7 egg chambers. **(C) Microvilli-specific atypical Cad99C localises beneath accumulated actin in CAP mutant cells**. Mosaic follicular epithelium with CAP mutant cells (GFP, pseudo-colored yellow, dashed line) stained for F-actin (phalloidin, magenta) and immunostaining against microvilli-specific

1139 atypical Cadherin, Cad99C (cyan). Zoomed-in inset (dotted box) highlights the retention of
1140 Cad99C (cyan), below the accumulated F-actin (magenta) and failure to reach the apical side
1141 of the follicle cells. Scale bar = 10 µm. **(D) Line scan intensity profile of Cad99C in control**
1142 **and CAP mutant cells**. The intensity profile of Cad99C is plotted for representative control
1143 (light cyan) and CAP mutant (dark cyan) cells, revealing a shift in Cad99C localisation at the
1144 apical region of CAP mutant cells**. (E) Comparative line scan of filamentous actin and**
1145 **Cad99C.** Mean line scan intensity profiles of F-actin (magenta) and Cad99C (cyan) for (E)
1146 control and (E') CAP mutant follicle cells. In (E'), the x-axis represents the distance from the
1147 basal side of the accumulated F-actin to normalise for the variation in the space occupied by
1148 the accumulated actin in the mutant. The dotted line marks the apical-most boundary of the
1149 follicle cells, just below the microvilli (which in control cells are Cad99C positive). Data are
1150 presented as mean ± SEM; n = 15 cells, N = 6 egg chambers. **(F) Rab11-positive endosomes**
1151 **localise beneath apical actin in CAP mutant cells**. Mosaic follicular epithelium with CAP
1152 mutant cells marked by the absence of nuclear RFP (nlsRFP negative, pseudo-colored
1153 yellow), expressing YFP-tagged Rab11(pseudo colored cyan), stained with phalloidin against
1154 F-actin. Zoomed-in inset (dotted box) shows that the apically accumulated F-actin halts the
1155 apical trafficking of Rab11 endosomes. The orange arrow highlights the Rab11-YFP
1156 localisation on the oocyte cortex, and the blue arrow highlights the localisation on the apical
1157 surface of the follicle cells (FC). Scale bar = 10 µm. **(G) Line scan intensity profile of Rab11**
1158 **in control and CAP mutant cells**. The intensity profile of Rab11-YFP is plotted for
1159 representative control (light cyan) and CAP mutant (dark cyan) cells, revealing a shift in Rab11
1160 localisation at the apical region of CAP mutant cells. **(H) Comparative line scan of**
1161 **filamentous actin and Rab11.** Combined line scan intensity profiles of F-actin (magenta) and
1162 Rab11-YFP (cyan) for (H) control and (H') CAP mutant follicle cells. In (H'), the x-axis
1163 represents the distance from the basal side of the accumulated F-actin to normalize for the
1164 variation in the space occupied by the accumulated actin in the mutant cells. The dotted line
1165 marks the apical boundary of the follicle cells, just below the microvilli. Data are presented as
1166 mean ± SEM; n = 20 cells, N = 6 egg chambers. **(I) Dynein accumulates basally to the actin**
1167 **accumulation.** Mosaic follicular epithelium with CAP mutant cells (GFP positive,
1168 pseudocoloured yellow) stained for F-actin (magenta) with phalloidin and immunostained
1169 against motor protein dynein heavy chain (Dynein-HC, pseudocoloured cyan). Zoomed-in
1170 inset (dotted box) shows the accumulation of Dynein beneath the apically accumulated F-
1171 actin. The orange arrow highlights the Dynein-HC localisation on the oocyte cortex, and the
1172 blue arrow highlights the Dynein-HC localisation on the apical surface of the follicle cells (FC).
1173 Scale bar = 10 µm. **(J) Line scan intensity profile of dynein in control and CAP mutant**
1174 **cells.** The intensity profile of Dynein heavy chain is plotted for representative control (light
1175 cyan) and CAP mutant (dark cyan) cells, revealing a shift in Dynein localisation at the apical
1176 region of CAP mutant cells. **(K) Comparative line scan of filamentous actin and dynein.**
1177 Mean line scan intensity profiles of F-actin (magenta) and Dynein (cyan) are presented for (K)
1178 control and (K') CAP mutant follicle cells. In (K'), the x-axis represents the distance from the
1179 basal side of the accumulated F-actin to normalise for the variation in the space occupied by
1180 the accumulated actin in the cells. The dotted line marks the apical boundary of the follicle
1181 cells, just below the actin-rich microvilli. Data are presented as mean ± SEM; n = 11 cells, N =
1182 4 egg chambers.

1183

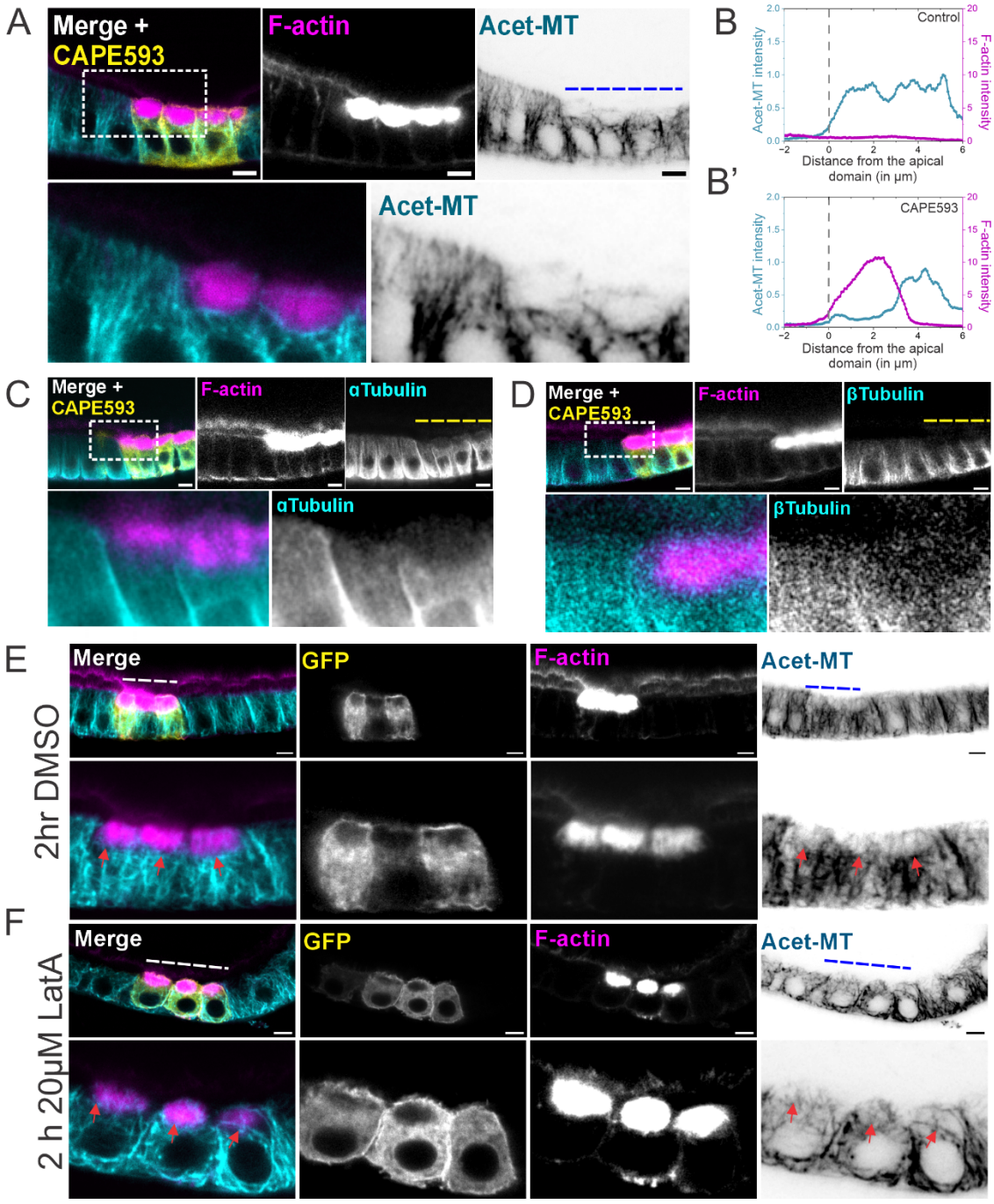

Figure 5. CAP loss of function results in F-actin accumulation and misorganized microtubules. (A) Apical actin accumulation excludes acetylated microtubules in CAP mutant follicle cells. A mosaic of follicular epithelium is shown, with CAP mutant cells highlighted by mCD8-GFP (GFP positive, pseudo-colored yellow, dashed line). The merged image illustrates the accumulation of filamentous actin at the apical region, as indicated by Phalloidin staining (pseudo-colored magenta). In contrast, acetylated microtubules (pseudo-coloured cyan) are absent from this region. Scale bar = 10 µm. Zoomed-in inset (dotted box) (Bertling et al., 2007)highlights the site of actin accumulation (magenta) devoid of acetylated microtubules. **(B) Line scan intensity profile** of the F-actin (magenta) and acetylated microtubules (cyan) for a single representative control (B) and CAP mutant follicle cell (B'). The dotted line marks the apical boundary of the follicle cells. **(C, D) Apical actin**

accumulation excludes microtubule α- and β-tubulin subunits in CAP mutant follicle cells (GFP positive, pseudo-colored yellow, dashed lines). Zoomed-in inset (dotted box) shows apical region CAP mutant cells with actin accumulation (Phalloidin, pseudo-colored magenta) and the site of apical actin accumulation is devoid of (C) α-Tubulin (cyan), and (D) β-Tubulin (cyan). Scale bar = 10 µm. **(E, F) Latrunculin A treatment fails to resolve dense accumulated actin of CAP mutant cells but facilitates microtubule entry.** Mosaic follicular epithelium with CAP mutant cells marked with mCD8-GFP (GFP positive, pseudo-colored yellow, dashed line), stained for filamentous actin (stained with phalloidin, pseudo-colored magenta) and for acetylated microtubules (Acet-MT, pseudo-colored cyan), treated with (E) DMSO (control) and (F) 20 µM Latrunculin A for 2 hours. In (E) DMSO-treated egg chambers, the site of actin accumulation lacked the microtubules. (F) Upon treatment with Latrunculin A, acetylated microtubules are seen at the site of actin accumulation and membrane-bound mCD8-GFP is also localised at the site of actin accumulation, showing partial disassembly of the accumulated actin. Scale bar = 10 µm.

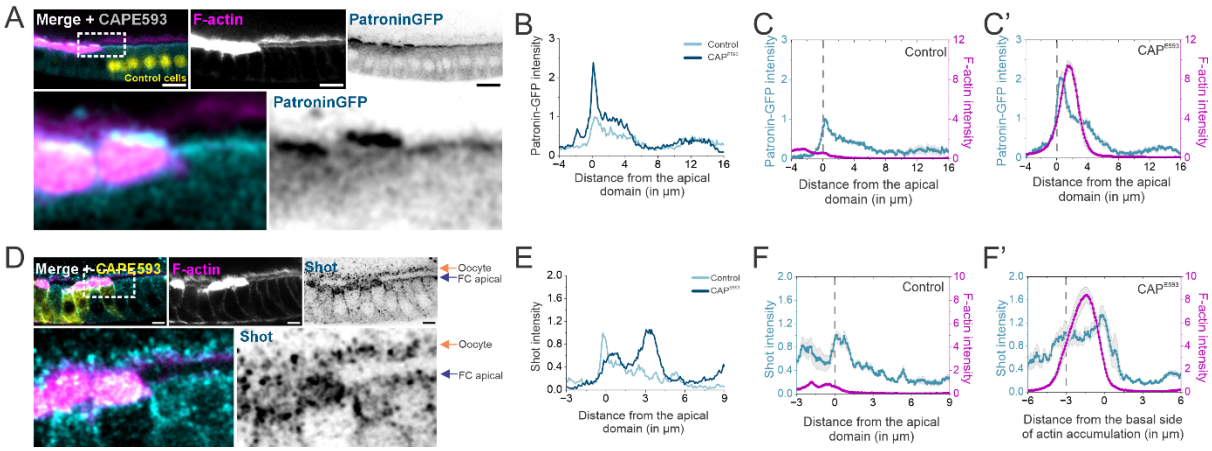

Figure 6. Localisation of microtubule minus-end anchoring proteins Patronin and actin-microtubule crosslinking protein Shot is impaired in CAP mutant cells. (A) Apical localisation of microtubule minus-end anchoring protein Patronin. Mosaic follicular epithelium with CAP mutant cells marked by the absence of nuclear RFP (nlsRFP (pseudocoloured yellow) negative) is shown. The merged image illustrates the accumulation of filamentous actin at the apical region, as indicated by Phalloidin staining (pseudo-colored magenta). Zoomed-in inset (dotted box), shows that the microtubule minus-end binding protein Patronin (Patronin-GFP, pseudo-colored cyan) is localized apically in both control cells (nlsRFP positive, pseudo-colored yellow) and CAP mutant cells (nlsRFP negative). However, the apical intensity of Patronin-GFP is higher in CAP mutant cells, and its localisation appears more diffuse. Scale bar = 10 µm. **(B) Line scan intensity profile of Patronin-GFP in control and CAP mutant cells.** The intensity profile of Patronin-GFP is plotted for representative control (light cyan) and CAP mutant (dark cyan) cells, revealing the increased localisation at the apical region of CAP mutant cells. **(C) Comparative line scan of filamentous actin and Patronin.** Mean line scan intensity profiles of F-actin (magenta) and Patronin-GFP (cyan) are presented for (C) control and (C') CAP mutant follicle cells. The dotted line marks the apical boundary of the follicle cells, just below the actin-rich microvilli. Data are presented as mean ± SEM; n = 5 cells, N = 3 egg chambers. **(D) Impaired apical localisation of actin-**

microtubule crosslinking protein Shot. Mosaic follicular epithelium with CAP mutant cells (GFP positive) staining F-actin (phalloidin) and antibody against Shot. The zoomed-in inset shows the disrupted apical localisation of actin-microtubule crosslinker Shot (pseudo-colored, cyan) at the site of actin accumulation. Shot is localised basal and around the accumulated actin. The orange arrow highlights the Shot localisation on the oocyte cortex, and the blue arrow highlights the localisation of Shot on the apical surface of the follicle cells (FC). Scale bar = 10 µm. **(E) Line scan intensity profile of Shot in control and CAP mutant cells**. The intensity profile of Shot is plotted for representative control (light cyan) and CAP mutant (dark cyan) cells, revealing a shift in Shot localisation at the apical region of CAP mutant cells. **(F) Comparative line scan of filamentous actin and Shot.** Combined line scan intensity profiles of F-actin (magenta) and Shot (cyan) for (F) control and (F') CAP mutant follicle cells. In (F'), the x-axis represents the distance from the basal side of the accumulated F-actin to normalize for the variation in the space occupied by the accumulated actin in the mutant cells. The dotted line marks the apical boundary of the follicle cells, just below the microvilli. Data are presented as mean ± SEM; n = 5 cells, N = 3 egg chambers.

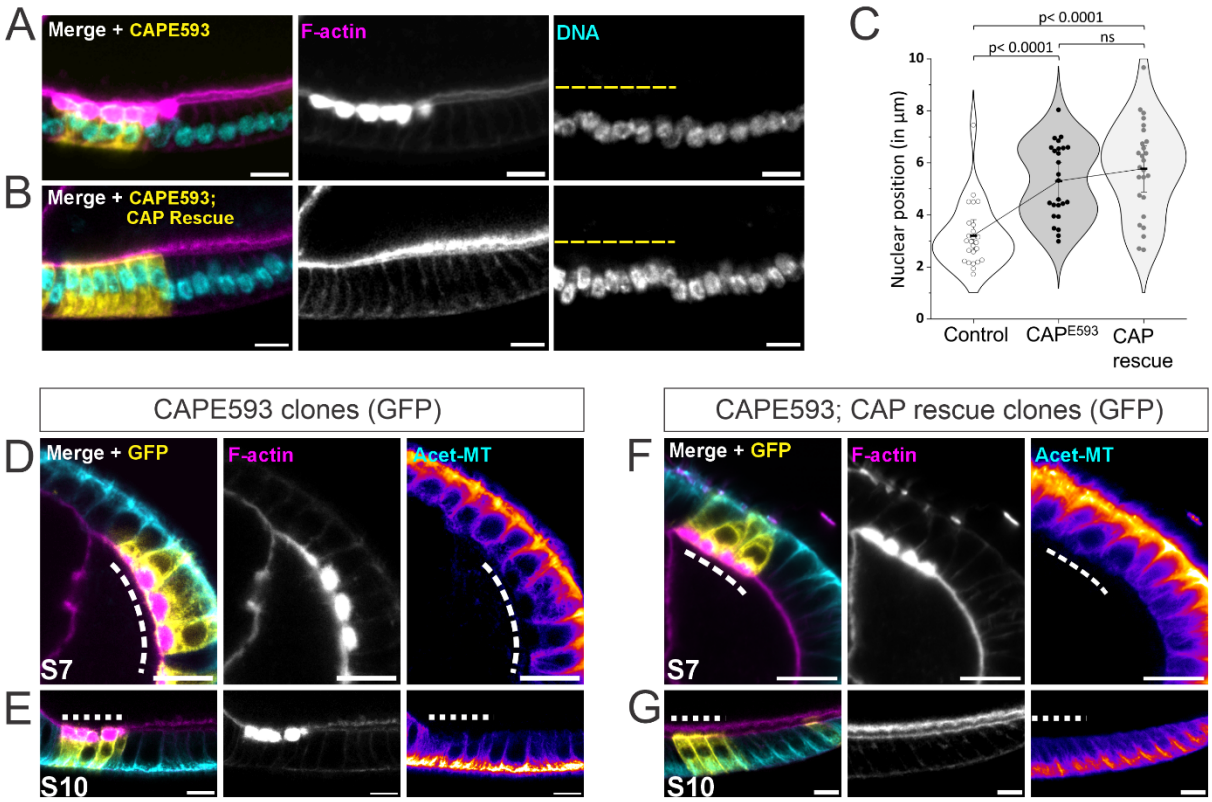

Figure 7. Apical actin accumulation during early oogenesis causes mispositioning of follicle cell nuclei. (A) CAP mutant cell nuclei are mispositioned apically. Mosaic follicular epithelium with CAP mutant cells marked with mCD8-GFP (GFP positive, pseudo-colored yellow, dashed line) and filamentous actin (stained with phalloidin, pseudo-colored magenta). In CAP mutant cells, nuclei (DNA stained with DAPI, pseudo-colored cyan) are positioned apically, while neighboring control cells (GFP negative) exhibit more basal nuclear positioning. Scale bar = 10 µm. **(B) Restoring CAP expression in CAP mutant cells rescues actin accumulation, but not the nuclear positioning phenotype.** Mosaic follicular epithelium with

1255 CAP mutant cells rescued by wild-type CAP expression (CAP rescue, GFP positive, pseudo-
1256 colored yellow, dashed line). While apical actin accumulation (filamentous actin stained with
1257 phalloidin, pseudo-colored magenta) is restored, the nuclei (DNA, cyan) remain mislocalized
1258 to the apical domain. Scale bar = 10 µm. **(C) Quantification of nuclear position in control,**
1259 **CAP mutant, and rescued cells.** A quantification graph is presented showing the nuclear
1260 position defined by the distance from the nucleus's center to the cell's basal side (in µm). The
1261 connecting line passes through the mean value of each group, and the whiskers represent the
1262 standard deviation. Kruskal–Wallis ANOVA followed by Dunn's post hoc test was used to
1263 assess the statistical significance of the different groups. Control = 25 cells, CAPE593 = 25
1264 cells, and CAP rescue = 26 cells. N = 6 egg chambers. **(D, E) CAP mutant cells display**
1265 **accumulated actin and microtubule disorganisation in both stage 7 and stage 10.** A
1266 cross-section of (D) stage 7 and (E) stage 10 mosaic follicular epithelium is shown, with CAP
1267 mutant cells highlighted by mCD8-GFP (GFP positive, dashed line). In both stages, CAP
1268 mutant cells display apical actin accumulation (filamentous actin stained with phalloidin,
1269 pseudo-colored magenta) and absence of acetylated microtubules (Acet-MT, pseudo-colored
1270 cyan). Scale bar = 10 µm. **(F) Actin accumulation and microtubule organization**
1271 **phenotypes are not rescued during early oogenesis.** A cross-section of stage 7 (s7)
1272 follicular epithelium, with CAP rescue clones highlighted by mCD8-GFP (GFP positive,
1273 pseudo-colored yellow, dashed line). The merged image demonstrates that apical actin
1274 accumulation is not rescued (filamentous actin stained with phalloidin, pseudo-colored
1275 magenta) nor is the organization of stable acetylated microtubules (Acet-MT, pseudo-colored
1276 cyan) in stage 7. Scale bar = 10 µm. **(G) Actin accumulation and microtubule organization**
1277 **phenotypes are successfully rescued in later stages of oogenesis.** A cross-section of
1278 stage 10 (s10) follicular epithelium is shown, with CAP wildtype rescue clones highlighted by
1279 mCD8-GFP (GFP positive, pseudo-colored yellow, dashed line). Both apical actin
1280 accumulation (filamentous actin stained with phalloidin, pseudo-colored magenta) and stable
1281 acetylated microtubules (Acet-MT, pseudo-colored cyan) are successfully restored. Scale bar
1282 = 10 µm.

1283

1284 **Table 1: CAP domain mutations**

Domains	Mutation	Reference	Function
HFD (90) Interface1	F122A, Y123A	(Kotila et al., 2019; Quintero-Monzon et al., 2009)(Kotila et al., 2019; Quintero-Monzon et al., 2009)(Kotila et al., 2019; Quintero-Monzon et al., 2009)	Cofilin-actin interaction Pointed end depolymerization
PP	^{179}PPPPPPP^{190} → ^{179}AAAAAAA^{190}		Profilin binding
WH2 (101)	K225A K226A	(Mattila et al., 2004)	ATP-actin binding
CARP (m6)	K315A N317A D322A	(Kotila et al., 2018)	ADP-actin binding, nucleotide exchange

1285

1286 **Table 2: *Drosophila* genotypes used**

Figure	Panel	Genotype	Abbreviation	Source
1	B	w1118	w1118	
	C-E	yw,hsFLP/w;TubGal80,FRT40A/Capt^{E593} FRT40A; TubP-GAL4, UAS-mCD8-GFP / +	CAP^{E593}	BDSC 5944
2	B	yw,hsFLP/w;TubGal80,FRT40A/Capt^{E593} FRT40A; TubP-GAL4, UAS-mCD8-GFP / +	CAP^{E593}	BDSC 5944
	C	yw,hsFLP/w;TubGal80,FRT40A/Capt^{E593} FRT40A; TubP-GAL4, UAS-Capt/ UAS-mCD8-GFP	CAP^{E593}; CAP Rescue	BDSC 5944 UAS-Capt, in this ms
	D	yw,hsFLP/w;TubGal80,FRT40A/Capt^{E593} FRT40A; TubP-GAL4, UAS-Captm6/ UAS-mCD8-GFP	CAP^{E593}; CARPmutant	BDSC 5944 UAS-Captm6, in this ms
	E	yw,hsFLP/w;TubGal80,FRT40A/Capt^{E593} FRT40A; TubP-GAL4, UAS-Chic/ UAS-mCD8-GFP	CAP^{E593}; ProfilinOE	BDSC 5944 Lynn Cooley
3	A, C, D, E	w,hsFLP/w; TubGal80, FRT40A/Capt^{E593} FRT40A; TubP-GAL4, UAS-mCD8-GFP / +	CAP^{E593}	BDSC 5944
	B	yw,hsFLP/w;TubGal80,FRT40A/Capt^{E593} FRT40A; TubP-GAL4, UAS-Capt/ UAS-mCD8-GFP	CAP^{E593}; CAP Rescue	UAS-Capt, in this ms
4	A, C, I	w,hsFLP/w; TubGal80, FRT40A/Capt^{E593} FRT40A; TubP-GAL4, UAS-mCD8-GFP / +	CAP^{E593}	BDSC 5944
	F	hsflp; UbimRFPnls, FRT40/Capt^{E593} FRT40A; Rab11EYFP/+	CAP^{E593}; Rab11YFP	BDSC 5944 BDSC 62549
	A	yw,hsFLP/w;TubGal80,FRT40A/Capt^{E593} FRT40A; TubP-GAL4, UAS-Capt/ UAS-mCD8-GFP	CAP^{E593}; CAP Rescue	BDSC 5944 UAS-Capt, in this ms
5	A, C-F	w,hsFLP/w; TubGal80, FRT40A/Capt^{E593} FRT40A; TubP-GAL4, UAS-mCD8-GFP / +	CAP^{E593}	BDSC 5944
6	A	hsflp;UbimRFPnls,FRT40/CaptE593 FRT40A; ubi.Patronin-GFP/+	CAP^{E593}; Patronin-GFP	BDSC 5944 BDSC 55129
	B	yw,hsFLP/w;TubGal80,FRT40A/Capt^{E593} FRT40A; TubP-GAL4, UAS-mCD8-GFP / +	CAP^{E593}	BDSC 5944
7	A, D, E	w,hsFLP/w;TubGal80,FRT40A/Capt^{E593} FRT40A; TubP-GAL4, UAS-mCD8-GFP / +	CAP^{E593}	BDSC 5944
	B, F, G	yw,hsFLP/w;TubGal80,FRT40A/Capt^{E593} FRT40A; TubP-GAL4, UAS-Capt/ UAS-mCD8-GFP	CAP^{E593}; CAP Rescue	BDSC 5944 UAS-Capt, in this ms.

1287